3121462

Ernst-Christian Koch

Metal-Fluorocarbon Based Energetic Materials

WILEY-VCH Verlag GmbH & Co. KGaA

662.2
K76m

The Author

Dr. Ernst-Christian Koch
NATO Munitions Safety
Information Analysis Center (MSIAC)
Boulevard Leopold III
1110 Brussels
Belgium

Cover
The cover picture depicts the combustion flame of Magnesium/Teflon TM/HycarTM strand (photographed by Andrzej Koleczko, Fraunhofer ICT, Germany) superimposed on the assumed main combustion step between difluorocarbene and magnesium.

All books published by **Wiley-VCH** are carefully produced. Nevertheless, authors, editors, and publisher do not warrant the information contained in these books, including this book, to be free of errors. Readers are advised to keep in mind that statements, data, illustrations, procedural details or other items may inadvertently be inaccurate.

Library of Congress Card No.: applied for

British Library Cataloguing-in-Publication Data
A catalogue record for this book is available from the British Library.

Bibliographic information published by the Deutsche Nationalbibliothek
The Deutsche Nationalbibliothek lists this publication in the Deutsche Nationalbibliografie; detailed bibliographic data are available on the Internet at <http://dnb.d-nb.de>.

© 2012 Wiley-VCH Verlag & Co. KGaA, Boschstr. 12, 69469 Weinheim, Germany

All rights reserved (including those of translation into other languages). No part of this book may be reproduced in any form – by photoprinting, microfilm, or any other means – nor transmitted or translated into a machine language without written permission from the publishers. Registered names, trademarks, etc. used in this book, even when not specifically marked as such, are not to be considered unprotected by law.

Cover Design Formgeber, Eppelheim
Typesetting Laserwords Private Limited, Chennai, India
Printing and Binding Markono Print Media Pte Ltd, Singapore

Printed in Singapore
Printed on acid-free paper

Print ISBN: 978-3-527-32920-5
ePDF ISBN: 978-3-527-64420-9
oBook ISBN: 978-3-527-64418-6
ePub ISBN: 978-3-527-64419-3
Mobi ISBN: 978-3-527-64421-6

1
Introduction to Pyrolants

Energetic materials are characterised by their ability to undergo spontaneous ($\Delta G < 0$) and highly exothermic reactions ($\Delta H < 0$). In addition, the specific amount of energy released by an energetic material is always sufficient to facilitate excitation of electronic transitions, thus causing known luminous effects such as glow, spark and flame. Energetic materials are typically classified according to their effects. Thus, they can be classified into high explosives, propellants and pyrolants (Figure 1.1). Typical energetic materials and some of the salient properties are listed in Table 1.1.

When initiated, high explosives undergo a detonation. That is a supersonic shockwave supported by exothermic chemical reactions [1–3]. In contrast, propellants and pyrolants undergo subsonic reactions and mainly yield gaseous products as in the case of propellants [4, 5] or predominantly condensed reaction products as in the case of pyrolants. The term *pyrolant* was originally coined by Kuwahara to emphasise on the difference between these materials and propellants [6]. Thus, the term aims at defining those energetic materials that upon combustion yield both hot flames and large amount of condensed products. Hence, pyrolants often find use where radiative and conductive heat transfer is necessary. Pyrolants also prominently differ from other energetic materials in that they have both very high gravimetric and volumetric enthalpy of combustion and very often densities far beyond $2.0\,g\,cm^{-3}$ (see Table 1.1 for examples).

Pyrolants are typically constituted from metallic or non-metallic fuels (e.g. Al, Mg, Ti, B, Si, $C_{(gr)}$ and S_8) and inorganic (e.g. Fe_2O_3, $NaNO_3$, $KClO_4$ and $BaCrO_4$) and/or organic (e.g. C_2Cl_6 and $(C_2F_4)_n$) oxidizers or alloying partners (e.g. Ni and Pd). In contrast to propellants, they are mainly fuel rich and their combustion is influenced by afterburn reactions with atmospheric oxygen or other ambient species such as nitrogen or water vapour.

Pyrolants serve a surprisingly broad spectrum of applications such as payloads for mine-clearing torches ($Al/Ba(NO_3)_2/PVC$) [7, 8], delays ($Ti/KClO_4/BaCrO_4$) [9], heating charges ($Fe/KClO_4$) [10, 11], igniters (B/KNO_3) [12, 13], illuminants ($Mg/NaNO_3$) [14, 15], thermites (Al/Fe_2O_3) [16, 17], obscurants ($RP/Zr/KNO_3$) (RP, red phosphorus) [18], ($Al/ZnO/C_2Cl_6$) [20], tracers ($MgH_2/SrO_2/PVC$) [21], initiators (Ni/Al) [22] and many more. Recently, pyrolant combustion is increasingly used for the synthesis of new materials.

Metal-Fluorocarbon Based Energetic Materials, First Edition. Ernst-Christian Koch.
© 2012 Wiley-VCH Verlag GmbH & Co. KGaA. Published 2012 by Wiley-VCH Verlag GmbH & Co. KGaA.

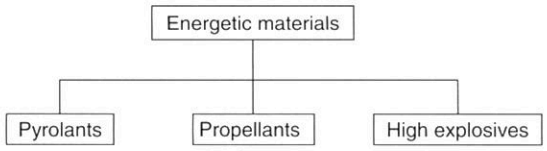

	Pyrolants	Propellants	High explosives
Process: Speed of reaction:	Burning Subsonic* <1 m s^{-1}	Deflagration Subsonic* 1–1000 m s^{-1}	Detonation Supersonic* >>1000 m s^{-1}
Reaction products:	Mainly condensed	Mainly gaseous	Mainly gaseous
Oxygen balance:	Fuel rich	Balanced	Balanced – Fuel rich
Combustion enthalpy:	1–30 kJ g^{-1} 5–50 kJ cm^{-3}	5–10 kJ g^{-1} 10–20 kJ cm^{-3}	5–15 kJ g^{-1} 15–25 kJ cm^{-3}
Density range:	2–10 g cm^{-3}	1.5–2.5 g cm^{-3}	<2 g cm^{-3} #)

* With respect to speed of sound of energetic material
#) Not taking into account metallized formulations and heavy metal based primary explosives

Figure 1.1 Classification of energetic materials.

Table 1.1 Performance parameters of selected energetic materials.

Class of energetic materials	Material, formula, weight ratio	ρ^a(g cm^{-3})	$\Delta_c H^c$ (kJ g^{-1})	$\Delta_c H^a$(kJ cm^{-3})	T_{ig}(°C)
High explosive	HMX, $C_4H_8N_8O_8$	1.906	9.459	18.028	287
	TNT, $C_7H_5N_3O_6$	1.654	14.979	24.775	300
	PETN, $C_5H_8N_4O_{12}$	1.778	8.136	14.465	148
	Nitroglycerine, $C_3H_5N_3O_9$	1.593	6.717	10.699	180
	Nitrocellulose[b], $C_6H_7N_3O_{11}$	1.660	9.118	15.135	200
Pyrolant	KNO_3/S_8/charcoal (75/10/15)	1.940	3.790	7.353	260–320
	Al/$KClO_4$(34/66)	2.579	9.780	25.223	446
	Fe/$KClO_4$ (20/80)	2.916	1.498	4.360	440–470
	Mg/PTFE/Viton (60/30/10)	1.889	22.560	42.616	540
	Zn/C_2Cl_6(45/55)	3.065	4.220	12.934	420
	Ta/THV-500[d] (74/26)	5.802	6.338	36.773	310

[a] At TMD = Theoretical Maximum Density.
[b] 14.4 wt% N.
[c] With liquid H_2O.
[d] THV-500 is copolymer of tetrafluoroethylene (TFE), Hexafluoropropene (HFP) and Vinylidene difluoride (VF_2) ratio: 60/20/20, $C_{2.223}H_{0.624}F_{3.822}$, $\rho = 2.03$ g cm^{-3}. PTFE, polytetrafluoroethylene.

An important group of pyrolants are those constituted from metal powder and halocarbon compounds [19]. The high energy density of metal–halocarbon pyrolants stems from the high enthalpy of formation of the corresponding metal–halogen bond (M–X). Thus, chlorocarbon but mainly fluorocarbon compounds are used as oxidizers.

On the basis of metal fluorocarbon combinations, pyrolants show superior exothermicity compared to many of the aforementioned fluorine-free systems [22]. This advantage is due to the high enthalpy of formation of the metal–fluorine bond not outperformed by any other combination of the respective metal. Thus, the exothermic step

$$M^w + wF \longrightarrow MF_w$$

is the driving force behind the reaction (w = maximum valence).

Owing to a great number of metallic elemental fluorophiles (~70), metal fluorocarbon pyrolants (MFPs) offer a great variability in performance. In addition, many alloys and binary compositions of fluorophiles may also come into play to further tailor the performance of the pyrolant: Mg_4Al_3, MgH_2, MgB_2, Mg_3N_2, $Mg(N_3)_2$, Mg_2Si and so on [23]. Very often MFPs find use in volume-restricted applications where other materials would not satisfy the requirements – see, for example, payloads for infrared decoy flares (see Chapter 10). Within the scope of this book, the following applications are discussed:

- agent defeat payloads
- countermeasure flares
- cutting torches
- heating devices
- igniters
- incendiaries
- material synthesis
- obscurants
- propellants
- reactive fragments
- stored chemical energy propulsion systems
- tracers
- tracking flares
- underwater flares.

This book focuses only on specialised pyrotechnic applications; thus, for a more generalised introduction to pyrotechnics, the interested reader is referred to the books by Shidlovski [24], Ellern [25], McLain [26], Conkling [27, 28], Hardt [29] and Kosanke *et al.* [30].

References

1. Fickett, W. and Davis, W.C. (2000) *Detonation – Theory and Experiment*, Dover Publications Inc., Mineola, New York.
2. Zukas, J.A. and Walters, W.P. (1998) *Explosive Effects and Applications*, Springer Publishers, New York.

3. Cooper, P.W. (1996) *Explosives Engineering*, Wiley-VCH Verlag GmbH, New York.
4. Kubota, N. (2007) *Propellants and Explosives, Thermochemical Aspects of Combustion*, 2nd completely revised and extended edn, Wiley-VCH Verlag GmbH, Weinheim.
5. Assovskiy, I.G. (2005) *Physics of Combustion and Interior Ballistics*, Nauka, Moscow.
6. Kuwahara, T. and Ochiai, T. (1992) Burning rate of magnesium/TF pyrolants. *Kogyo Kayaku*, **53** (6), 301–306.
7. Kannberger, G. (2005) Test and Evaluation of Pyrotechnical Mine Neutralisation Means. ITEP Work Plan Project Nr. 6.2.4, Final Report, Bundeswehr Technical Center for Weapons and Ammunition (WTD 91), Germany.
8. N.N. (2005) *Operational Evaluation Test of Mine Neutralization Systems*, Institute for Defense Analyses, Alexandria, http://en.wikipedia.org/wiki/Political_divisions_of_the_United_States VA.
9. Wilson, M.A. and Hancox, R.J. (2001) Pyrotechnic delays and thermal sources. *J. Pyrotech.*, **13**, 9–30.
10. Callaway, J., Davies, N. and Stringer, M. (2001) Pyrotechnic heater compositions for use in thermal batteries. 28th International Pyrotechnics Seminar, Adelaide Australia, November 4–9, 2001, pp. 153–168.
11. Czajka, B. and Wachowski, L. (2005) Some thermochemical properties of high calorific mixture of Fe-$KClO_4$. *Cent. Eur. J. Energetic Mater.*, **2** (1), 55–68.
12. Klingenberg, G. (1984) Experimental study on the performance of pyrotechnic igniters. *Propellants Explos. Pyrotech.*, **9** (3), 91–107.
13. Weiser, V., Roth, E., Eisenreich, N., Berger, B. and Haas, B. (2006) Burning behaviour of different B/KNO_3 mixtures at pressures up to 4 MPa. 37th International Annual ICT Conference, Karlsruhe Germany, June 27–30, p. 125.
14. Beardell, A.J. and Anderson, D.A. (1972) Factors affecting the stoichiometry of the magnesium-sodium nitrate combustion reaction. 3rd International Pyrotechnics Seminar, Colorado Springs, CO, 21–25 August, pp. 445–459.
15. Singh, H., Somayajulu, M.R. and Rao, B. (1989) A study on combustion behaviour of magnesium – sodium nitrate binary mixtures. *Combust. Flame*, **76** (1), 57–61.
16. Fischer, S.H. and Grubelich, M.C. (1998) Theoretical energy release of thermites, intermetallics, and combustible metals. 24th International Pyrotechnics Seminar, Monterey CA, July 27–31, pp. 231–286.
17. Weiser, V., Roth, E., Raab, A., del Mar Juez-Lorenzo, M., Kelzenberg, S. and Eisenreich, N. (2010) Thermite type reactions of different metals with iron-oxide and the influence of pressure. *Propellants Explos. Pyrotech.*, **35** (3), 240–247.
18. Koch, E.-C. (2008) Special materials in pyrotechnics: V. Military applications of phosphorus and its compounds. *Propellants Explos. Pyrotech.*, **33** (3), 165–176.
19. Koch, E.-C. (2010) *Handbook of Combustion*, Wiley-VCH Verlag GmbH, pp. 355–402.
20. Ward, J.R. (1981) MgH_2 and $Sr(NO_3)_2$ pyrotechnic composition. US Patent 4, 302,259, USA.
21. Gash, A.E., Barbee, T. and Cervantes, O. (2006) Stab sensitivity of energetic nanolaminates. 33rd International Pyrotechnics Seminar, Fort Collins CO, July 16–21, pp. 59–70.
22. Cudzilo, S. and Trzcinski, W.A. (2001) Calorimetric studies of metal/polytetrafluoroethylene pyrolants. *Pol. J. Appl. Chem.*, **45**, 25–32.
23. Koch, E.-C., Weiser, V. and Roth, E. (2011) Combustion behaviour of binary pyrolants based on MgH_2, MgB_2, Mg_3N_2, Mg_2Si, and polytetrafluoroethylene. EUROPYRO 2011, Reims, France, May 16–19.
24. Shidlovski, A.A. (1965) Fundamentals of Pyrotechnics.
25. Ellern, H. (1968) *Military and Civilian Pyrotechnics*, Chemical Publishing Company, New York.

26. McLain, J.H. (1980) *Pyrotechnics from the Viewpoint of Solid State Chemistry*, The Franklin Institute Press, Philadelphia, PA.
27. Conkling, J. (1985) *Chemistry of Pyrotechnics – Basic Principles and Theory*, Marcel Dekker, Inc., Basel.
28. Conkling, J. and Mocella, C.J. (2011) *Chemistry of Pyrotechnics – Basic Principles and Theory*, CRC Press, Boca Raton, FL.
29. Hardt, A. (2001) *Pyrotechnics*, Pyrotechnica Publications, Post Falls, ID.
30. Kosanke, K., Kosanke, B., Sturman, B., Shimizu, B., Wilson, A.M., von Maltitz, I., Hancox, R.J., Kubota, N., Jennings-White, C., Chapman, D., Dillehay, D.R., Smith, T. and Podlesak, M. (2004) *Pyrotechnic Chemistry*, Pyrotechnic Reference Series, Journal of Pyrotechnics Inc., Whitewater, CO.

The French forces applied these obscurants in the First World War with both navy and army in the so-called smoke generators. Later in the war, the Berger mixture saw widespread application with all belligerent countries. Berger was honored with the "Grand Prix de la Marine" in 1918 for his contribution to French warfare [14]. After the war, Berger reported that he had been in contact with Victor Grignard by early 1916 on these mixtures. Grignard had also proposed to him to use hexachlorobenzene as an alternative source of chlorine. In the same report, Berger also refers to Matignon's work [14]. Thus, it is very likely that he was inspired to apply these highly exothermic reactions in pyrotechnic obscurant formulations [15].

In 1919, the US First World War veteran Richard Clyde Gowdy (1886–1946), a citizen of Cincinatti, invented a signal smoke mixture based on magnesium, hexachloroethane, and anthracene [17]. Although Berger had already proposed to use magnesium as a fuel, it was noted by him that these mixtures would burn almost too vigorously. Gowdy, a mechanical engineer, modified Berger's mixture in that he applied anthracene both to cool down the combustion temperature and to generate soot that would turn the generated smoke black. It can be assumed that Gowdy learned about the Berger mixture in his military deployment to Europe.

Further refinements and modifications of Berger's smoke mixture were successively undertaken by Metivier (1926) [18, 19] and Brandt (1937) [20] both in France.

In 1922, Staudinger reported about explosive reactions of alkali and alkaline earth metals with partially and perhalogenated solvents such as CH_2Cl_2 and CCl_4. He intuitively assumed the formation of a very instable species on contact that would be very sensitive to mechanical impact and thus trigger an explosive reaction. However, he was unable to identify the actual species [21] but proposed to exploit these fierce reactions in detonating charges for ammunition [22, 23]. Staudinger was a visionary and he even tried to apply the explosive reaction between sodium and tetrachloromethane to make diamond [24]. He thought that both the high temperature and pressure from the explosion would enable to force the formed carbon soot to undergo phase transition to diamond. Although he was not successful with his experiment, about 60 years later nanodiamonds were isolated from TNT/RDX detonation soot and proved Staudinger's basic idea that a detonation would furnish the necessary physical conditions for the formation of diamond [25]. Still 10 years after that (in 1998), a Chinese group reported about the successful nanodiamond synthesis based on the original Staudinger set up with sodium and tetrachloromethane in an autoclave [26].

2.3 Rise of Fluorocarbons

In the course of the electrolytic preparation of beryllium from molten KHF_2/BeF_2, in 1926, Paul Lebeau (1858–1959) and his collaborator Damien were able to purify and isolate tetrafluoromethane, CF_4, by fractional distillation with a liquid air-cooled condenser. They observed vigorous combustion reactions of CF_4 with both sodium and calcium [27].

In 1930, Otto Ruff (1871–1939) and his coworker Otto Bretschneider synthesized CF_4 by a reaction of F_2 with charcoal and reported about violent combustion reactions of tetrafluoromethane with both calcium and magnesium at elevated temperatures [28]. Ruff and Brettschneider were also the first to obtain the important monomer tetrafluoroethylene, C_2F_4 (TFE), from tetrafluoromethane by arc discharge between graphite electrodes (Scheme 2.1) in 1933. They described its fierce combustion reaction with sodium [29].

Scheme 2.1 TFE synthesis via arc discharge between carbon electrodes.

In 1934, Ruff and Brettschneider synthesized the first *all*-fluorinated polymer, graphite fluoride, $(CF_x)_n$, by fluorination of norite (Scheme 2.2) and investigated its thermal stability and decomposition mechanisms [30].

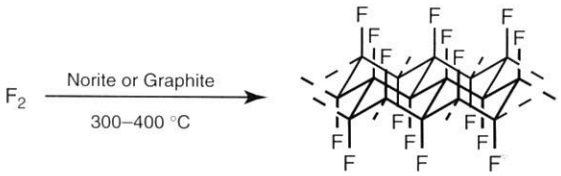

Scheme 2.2 Synthesis of graphite fluoride by fluorination of norite or graphite.

The first ever reported fluorinated flexible polymers based on fluorinated ethylenes were developed in 1934 by Fritz Schloffer (1901–1978) and Otto Scherer (1903–1987), both were from IG Farben/Frankfurt Germany. They described polymerization of chlorotrifluoroethylene to give polychlorotrifluoroethylene, $(CF_2ClF)_n$, according to Scheme 2.3 [31].

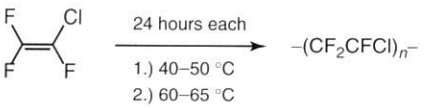

Scheme 2.3 Polymerization of chlorotrifluoroethylene (CTFE) according to Ref. [31].

They also described the synthesis of polychlorodifluoroethylene, $(CClHCF_2)_n$, polybromotrifluoroethylene $(CBrFCF_2)_n$, and mixed polyvinylchloride-*co*-polychlorotrifluoroethylene $(CClFCF_2)_m(CH_2CHCl)_n$, where all these occur under similar reaction conditions. Mass production of these started shortly after that. Later these materials were adopted in the United States by Kellog Company and marketed under the brand name Kel-F®. Former Hoechst scientist Walter Wetzel (born 1925) in his paper on the discovery of polytetrafluoroethylene (PTFE) has revealed, from the company archives of Hoechst, that Schloffer and Scherer had investigated the polymerization of TFE as well but the resulting polymer, PTFE,

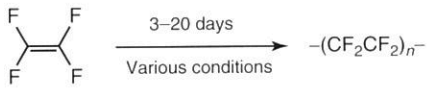

Scheme 2.4 Polymerization of TFE according to Ref. [33].

owing to its chemical inertness and insolubility was not considered a useful material [32]. The application department at Hoechst rejected the material with the rather rhetoric question: "Was sollen wir mit diesem klitschigen Ding?" literally translated: "What do you expect us to do with this repellent material?" In view of the problems to access technical reasonable quantities of TFE to run into mass production – a technical problem that should remain for another 15 years – Hoechst unfortunately decided to disregard this material and did not include PTFE in the upcoming disclosure [31].

In 1939, Roy Plunkett (1911–1994) at Dupont discovered the polymerization of TFE to give PTFE the chemically and thermally most resistant fluoropolymer ever made (Scheme 2.4) [33]. However, similar to Schloffer's and Scherer's experience with the same material, Plunkett would not obtain any royalties from Dupont as the company would not work on PTFE for another four years for the same reasons [32]. It was only in 1943 when the Manhattan project created a demand for corrosion-resistant liners and gasket for reactors and valves to handle highly corrosive UF_6 [34]. Then, people at Dupont remembered the highly hydrophobic and chemically inert material. This is when PTFE came into play again and its small-scale production started. At the end of the 1940s, PTFE was produced on a small scale for the civilian market under the brand name Teflon®.

From a BIOS report, it is known that successive chlorination and fluorination of "Cerisin," a hydrocarbon wax frequently used in Germany, was applied before the war to obtain chemically highly resistive waxes with 57 wt% chlorine and 20 wt% fluorine for chemical engineering purposes [35].

In addition, in 1939, Hugo Stoltzenberg (1883–1974) invented a new obscurant based on magnesium and a mixture of liquid and solid halocarbon compounds [36]. His company was one of the few private firms beside big IG Farben to be involved with the complete span of chemical warfare development in Germany. He developed all kinds of warfare supplies for German Wehrmacht such as pyrotechnics (illuminants, obscurants, and incendiaries), chemical warfare agents, and the corresponding protective equipment. Thus, he had the most advanced materials such as the newly invented fluoropolymers at his disposal. Hence, it is likely that he had experimented with them as oxidizers as well. At the time of writing this book, any of the FIAT/CIOS/BIOS[1] interrogation files of Hugo Stoltzenberg were still not released by either UK or US government (*sic*).

1) Combined Intelligence Objectives Subcommittee (CIOS), British Intelligence Objectives Subcommittee (BIOS), Field Information Agency Technical (FIAT) are allied post-war reports on German Science and Industry.

to the PbS ($\lambda = 1.9–2.6\ \mu m$) and PbTe ($\lambda = 3.2–5.1\ \mu m$) spectral detector range is given below.

SR 107 [46]	SR 580 [46]
Composition	
35 wt% Magnesium	60 wt% Magnesium
65 wt% Ferric oxide	36 wt% Sodium nitrate
	4 wt% Acaroid resin
Spectral efficiency	
E_{PbS}: 56 J g^{-1} sr^{-1}	E_{PbS}: 21 J g^{-1} sr^{-1}
E_{PbTe}: 31 J g^{-1} sr^{-1}	E_{PbTe}: 10 J g^{-1} sr^{-1}
Spectral radiance	
L_{PbS}: 33 W sr^{-1} cm^{-2}	L_{PbS}: 27 W sr^{-1} cm^{-2}
L_{PbS}: 18 W sr^{-1} cm^{-2}	L_{PbS}: 18 W sr^{-1} cm^{-2}

2.5 Metal/Fluorocarbon Pyrolants

The first unambiguously documented use of fluorocarbon as oxidizers in pyrotechnics was 1956 in a patent that was not published until 1964. The chemist Edgar A. Cadwallader (1918–2006) disclosed the first pyrotechnic material to include a fluoropolymer, Kel-F, polychlorotrifluoroethylene, and a metal such as magnesium or aluminium for a visual flare composition (Table 2.2) [47].

Cadwallader had worked on organometallic reactions previously [48], obviously a prerequisite for many researchers involved with metal–halocarbon reactions. The first reported use of a metal/fluorocarbon material in infrared tracking flares then was made in Spring 1956. At NOTS, the type 702A target augmentation flare was designed, which used the below given composition based on Mg and PTFE [49]. The flare material had a heat of reaction of 9.2 kJ g^{-1} and a specific energy in the PbS band that would outperform both SR 107 and 580 by two or six times.

Table 2.2 Table with ingredient proportions and performance of a 0.5 in diameter flare candle. (Taken from Cadwallader's disclosure [47].)

Mg (%)	Kel-F (%)	Candle power
40	60	18
50	50	19
60	40	25
70	30	40

er details of
/inder A-1

rain Detector

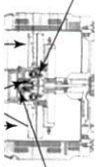

Reticle

seeker unit.

ırpose, however,
sic metal/nitrate
perchlorate [44]
ish illuminating
se compositions

was SR 107 [46].
s corresponding

Name of flare	Composition	Watts/ steradian per Sq. In. Burning Surface (0.8 – 3.5 μm) Ambient	65 000 Feet
1. BuOrd Mk 21 Mk O	54% Mg 34% $NaNo_3$ 12% Laminac	677	500
2. Applicants' flare	54% Mg 23% Teflon 23% Kel-F	2283	1070
3. Army "Rita" flare	66.7% Mg 28.5% $NaNO_3$ 4.8% Binder	1000	—
4. Optimum aluminum-Teflon	48% Al 52% Teflon	1700	—
5. Optimum boron-Teflon	56% B 44% Teflon	445	—
6. Optimum zirconium-Teflon	54% ZrH_2 46% Teflon	428	—

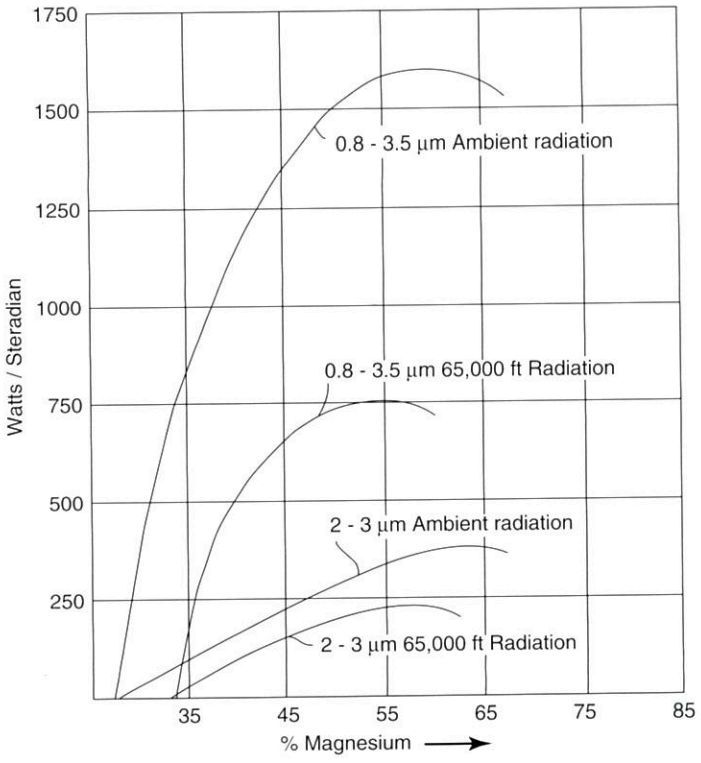

Figure 2.6 Ingredient proportions and performance of an infrared flare candle. (Taken from Hahn's disclosure [45].)

NOTS 702 [49]
54 wt% Magnesium
30 wt% Polytetrafluoroethylene
16 wt% Kel-F wax
Performance
$E_{1.8-2.7\mu m}$: 125 J g^{-1} sr^{-1}
Burn rate: 3.4 mm s^{-1}
$I_{1.8-2.7\mu m}$: 300 W sr^{-1}

A similar composition was finally filed by Hahn, Rivette, and Weldon in a patent application in 1958, which was not disclosed until nearly 39 years later in 1997 [45].

The spectral performance in both 2–3 μm band is given in Figure 2.6.

A report on magnesium/Teflon®/Kel-F-based infrared flare compositions and their performance was issued in 1959 and declassified from secret to unclassified in 1980 [50].

In 1962, Hugo Stoltzenberg and his coworker Martin Leuschner (1913–1982) filed a patent on obscurants based on titanium and fluorocarbons and/or chlorocarbons that was published in 1965 [51]. In 1963, the IIT Research Institute located in Illinois Chicago issued a report under Air-Force contract on thermochemical properties of a large number of metal/oxidizer systems. Their considerations also included both CF_4 and C_2F_6 as oxidizers [52].

In 1965, the Russian chemist Alexander Alexandrovich Shidlovskii (1911–1985) in his book on pyrotechnics refers to the possibility to use PTFE as an oxidizer in pyrotechnic mixtures [53]. Finally, Herbert Ellern (1902–1987) in his epochal monograph on pyrotechnics in 1968 for the first time in the open and accessible literature refers to the use of magnesium/PTFE mixtures in infrared decoy flares and gives details on caloric data and ignition sensitivity [54]. From then on, magnesium/PTFE has made its way into numerous applications as will be discussed in the following chapters.

References

1. *http://de.wikipedia.org/w/index.php?title=Datei:Edward_Frankland.jpg&filetimestamp=20050608204915* (accessed September 1 2011).
2. Frankland, E. (1848) Ueber die Isolirung der organischen Radicale. *Ann. Chem.*, **71**, 171–213.
3. Wurtz, C.A. (1855) Sur une nouvelle classe de radicaux organiques. *Ann., Chim., Phys.*, **44**, 275–312.
4. Hallwachs, W. and Schafarik, A. (1859) Ueber die Verbindungen der Erdmetalle mit organischen Radicalen. *Liebigs Ann. Chem.*, **109**, 206–109.
5. Moissan, H. (1886) Nouvelles experiences sur la decomposition de l'acide fluorhydrique par un courant electrique. *Comptes rendus hebdomadaires des séances de l'Académie des sciences*, **103**, 256–258.
6. Moissan, H. (1890) Sur la preparation et les proprietes du tetrafluorure de carbone. *Comptes rendus hebdomadaires des séances de l'Académie des sciences*, **110**, 951–954.
7. Barbier, P. (1899) Synthese du demethylheptenol. *Comptes rendus hebdomadaires des séances de l'Académie des sciences*, **128**, 110–111.

8. Grignard, V. (1900) Sur quelques nouvells combinaisons organometalliques du magnesium et leur application a des syntheses d'alcools et d'hydrocarbures. *Comptes rendus hebdomadaires des séances de l'Académie des sciences*, **130**, 1322–1324.
9. Rieke, R.D. and Hudnall, P.M. (1972) Activated metals. I. Preparation of highly reactive magnesium metal. *J. Am. Chem. Soc.*, **94**, 7178–7179.
10. Matignon, C. (1907) Formation et preparation du carbure d'aluminium. *Comptes rendus hebdomadaires des séances de l'Académie des sciences*, **145**, 676–679.
11. Staudinger, H. and Anthes, E. (1913) Oxalylchlorid. V.: Über Oxalylbromid und Versuche zur Darstellung von Di-kohlenoxid. *Chem. Ber.* **46**, 1426–1437.
12. Bret, P. (2006) Les Laboratoires Français et l'étude des Munitions et Matériels Allemands Pendant la Grande Guerre, Cahier du CEHD, No. 33, Les relations Franco-Allemande.
13. Hanslian, R. (1937) *Der Chemische Krieg, I. Militärischer Teil*, Verlag von E.S. Mittler & Sohn, Berlin, p. 630.
14. Berger, E. (1920) Production de chlorures par reactions amorcees. *Comptes rendus hebdomadaires des séances de l'Académie des sciences*, **171**, 29–32.
15. Berger, E. (1919) Noveau procede, D'obtention de fumees par combustion des melanges. FR Patent 501,836, filed Nov. 1, 1916, France.
16. Berger, E.-E.-F. (1920) Nouveau procede d'obtention de fumes par combustion de mélanges. FR Patent 501,836 1ere addition, France.
17. Gowdy, R.C. (1919) Smoke-making compound for signal rocket. US Patent 1,318,074, filed April 24, 1919, USA.
18. Metivier, M. (1926) Engins fumigenes a l'ethane hexachlore et aux derives chlores du naphthalene. FR Patent 613,884.
19. Metivier, M.-A.-E. (1928) Engins funigenes a l'ethane hexachlore au propane octochlore et aux derives chlores du naphthalenes: engins ordinaries, engins a flotteur. FR Patent 649,853.
20. Brandt, E.W. (1937) Artifice fumigene. FR Patent 807,502, France.
21. Staudinger, H. (1922) Erfahrungen über einige Explosionen, *Angew. Chem.*, **35**, 657–659.
22. Staudinger, H. (1922) Verfahren zur Initialzündung von Sprengstoffen. DE 391,346, Deutschland.
23. Staudinger, H. (1922) Verfahren zur Herstellung von Sprengmitteln. DE Patent 396,209, Deutschland.
24. Staudinger, H. (1961) *Arbeitserinnerungen*, Hüthig Verlag, Heidelberg.
25. Greiner, R.N., Phillips, D.S., Johnson, J.D. and Volk, F. (1988) Diamonds in detonation soot. *Nature*, **333**, 440–442.
26. Li, Y., Qian, Y., Liao, H., Ding, Y., Yang, L., Xu, C., Li, F. and Zhou, G. (1998) A reduction-pyrolysis-catalysis synthesis of diamond. *Science*, **281**, 246–247.
27. Lebeau, P. and Damiens, A. (1926) Sur le tetrafluorure de carbone, *C. R. Acad. Sci.* **182**, 1340–1342.
28. Ruff, O. and Keim, R. (1930) Die Reaktionsprodukte der verschiedenen Kohlearten mit Fluor. I. Das Kohlenstoff-4-fluorid (Tetrafluormethan). *Z. Anorg. Allg. Chem.*, **192**, 249–256.
29. Ruff, O. and Bretschneider, O. (1933) Die Bildung von Hexafluorethan und Tetrafluoräthylen aus Tetrafluorkohlenstoff. *Z. Anorg. Allg. Chem.*, **210**, 173–183.
30. Ruff, O. and Bretschneider, O. (1934) Die Reaktionsprodukte der verschiedenen Kohlearten mit Fluor. II (Das Kohlenstoff-monofluorid). *Z. Anorg. Allg. Chem.*, **217**, 1–18.
31. Schloffer, F. and Scherer, O. (1939) Verfahren zur Darstellung von Polymerisationsprodukten. DE Patent 677,071, Filed Oct. 7, 1934, Germany.
32. Wetzel, W. (2005) Entdeckungsgeschichte der Polyfluorethylene–Zufall oder Ergebnis gezielter Forschung? *NTM Z. Gesch. Wissen. Tech. Med.*, **13**, 79–91.
33. Plunkett, R. (1939) Tetrafluoroethylene polymers. US Patent 2,230,654, USA.
34. Kirsch, P. (2004) *Modern Fluoroorganic Chemistry: Synthesis, Reactivity, Applications*, Wiley-VCH Verlag GmbH, Weinheim.

35. British Intelligence Objectives Sub-Committee (BIOS) (1946) German Fluorine and Fluoride Industry, Final Report 1595, Item No. 22.
36. Stoltzenberg, H. (1942) Verfahren zur Herstellung von Magnesiumhalogenidnebeln. DE Patent 724,807, Deutschland.
37. Lusar, R. (1964) *Die deutschen Waffen und Geheimwaffen des 2. Weltkrieges und ihre Weiterentwicklung*, 5th edn, J. F. Lehmann, München.
38. Zippermayr, M. (1945) Testimony Given Towards CIOS Mission 214 "Salzburg Area".
39. Simon, L.E. (1971) *German Research in World War II*, WE Inc. Publishers, Old Greenwich, p. 11, 23, 126.
40. Simon, L.E. (1947) *German Scientific Research Establishments*, Mapleton House, New York, p. 162.
41. Pick, H. (1948) Über lichtelektrische Leitung am Bleisulfid. *Ann. Phys.*, **3**, 255–269.
42. Blanchard, D.G. (1996) A brief history of air-intercept missile 9 (Sidewinder). 32nd Joint Propulsion Conference, Lake Buena Vista, FL, 1–3 July, AIAA-1996-3154.
43. *http://en.wikipedia.org/wiki/File:2008-12_mclean_ship_name01.jpg*, (accessed September 1 2011).
44. Loedding, A.C. (1958) Tracking flares. US Patent 2,829,596, filed 1954.
45. Hahn, G.T., Rivette, P.G. and Weldon, R.G. (1997) Infra-red tracking flare. US Patent 5,679,921, filed 1958, USA.
46. Moss, T.S., Brown, D.R. and Hawkins, T.D.F. (1957) Infra-Red Decoys, Technical Note No. RAD.702 Royal Aircraft Establishment, September 1957.
47. Cadwallader, E.A. (1964) Flare composition. US Patent 3,152,935, filed 1956, USA.
48. Cadwallader, E.A., Fookson, A., Mears, T.W. and Howard, F.L. (1948) Aliphatic halide-carbonyl condensations by means of sodium. *J. Res.*, **41**, 111–118.
49. Tyroler, J.F. and Knapp, C.A. (1957) An Evaluation of the NOTS Type 702A Infrared, Picatinny Arsenal, PL-R-TN No. 6, 25 October 1957.
50. Knapp, C.A. (1959) *New Infrared Flare and High Altitude Igniter Compositions*, Feltman Research and Engineering Laboratories, Picatinny Arsenal, Dover, NJ.
51. Stoltzenberg, H. and Leuschner, M. (1965) Nebelsatz zur Herstellung von beständig gefärbten anorganischen Nebeln, DE Patent 1,188,490, filed 1962, Deutschland.
52. Raisen, E., Katz, S. and Franson, K.D. (1963) *Survey of the Thermochemistry of High-Energy Reactions*, IIT Research Institute, Chicago, IL, Prepared under Contract No. AF 33(616)-7835.
53. Shidlovskii, A.A. (1965) Fundamentals of Pyrotechnics, Technical Memorandum 1615, Translated by U.S. Joint Publication Research Service from a Russian Textbook. Osnovy Pirotekhniki issued in 1964.
54. Ellern, H. (1968) *Military and Civilian Pyrotechnics*, Chemical Publishing Company, New York, p. 412.

Further Reading

Douda, B.E. (2009) *Genesis of Infrared Decoy Flares*, Naval Surface Warfare Center, Crane, IN.

Henne, A.L. and Renoll, M.W. (1936) Fluoroethanes and fluoroethylenes. *V. J. Am. Chem. Soc.*, **58**, 889–890.

Julian, E.C., Crescenzo, F.G. and Meyers, R.C. (1973) Igniter composition. US Patent 3,753,811, filed 1957, USA.

3
Properties of Fluorocarbons

3.1
Polytetrafluoroethylene (PTFE)

Polytetrafluoroethylene (PTFE) is a crystalline translucent solid polymer with a high molecular weight ranging between 10^6 and 10^7 g mol^{-1}. It is prepared from the monomer C_2F_4 by polymerization in aqueous medium and is obtained as fine powder. A number of trade names exist for PTFE. Thus it is often referred to as *Teflon® (DuPont), Hostaflon® (Dyneon), Fluon® (ICI), Halon® (Allied Chemical)* or *Fluoroplast® (Ftoroplastoviye Tekhnologii JSC)* [1, 2].

PTFE undergoes a series of first- and second-order transitions at 19 °C (first), 30 °C (second) and 90 °C (first), and finally at 130 °C (second), it expands to about 1.2 times its volume. At 340 °C, pristine PTFE changes into a transparent amorphous gel and expands to about 1.3 times its solid state volume [1]. However, this melt process is irreversible, and remelting of the recrystallized polymer will occur at 327 °C [1]. At temperatures above 350–400 °C, pyrolysis of the polymer into gaseous products occurs. This occurs without significant charring, as the C–C bond is significantly weaker (348 kJ mol^{-1}) than the C–F bond (507 kJ mol^{-1}), thus favouring C–C scission over C–F bond breaking [3, 4]. The main decomposition products of PTFE are tetrafluoroethylene (TFE) and CF_2, which depending on the reaction conditions undergo successive reactions and yield complex product mixtures [4]. Hydrogen and chlorine atmosphere inhibit PTFE decomposition, whereas steam, oxygen and sulfur dioxide accelerate its decomposition [4]. The thermal decomposition in moist air yields carbonyl difluoride, CO_2F and the monomer [5, 6]. The monomer itself will also undergo further reaction to both carbonyl difluoride and difluorocarbene. In the presence of moisture, both carbonyl difluoride and difluorocarbene give hydrofluoric acid and carbon dioxide or monoxide [5].

$$(C_2F_4)_n \xrightarrow[\text{Air}]{\Delta} n\,COF_2 + \frac{n}{2}\,C_2F_4 \tag{3.1}$$

$$C_2F_4 \xrightarrow[\text{Air}]{\Delta} COF_2 + CF_2 \tag{3.2}$$

$$COF_2 + H_2O \longrightarrow 2\,HF + CO_2 \tag{3.3}$$

$$CF_2 + H_2O \longrightarrow CO + 2\,HF \tag{3.4}$$

Metal-Fluorocarbon Based Energetic Materials, First Edition. Ernst-Christian Koch.
© 2012 Wiley-VCH Verlag GmbH & Co. KGaA. Published 2012 by Wiley-VCH Verlag GmbH & Co. KGaA.

Table 3.1 Main products of pyrolysis of PTFE.

Products	Formula	Unit	Temperature (°C)		
			605	650	700
Tetrafluoroethylene	C_2F_4	weight percentage	78.5	75.0	60.2
Hexafluoropropene	C_3F_6	weight percentage	4.6	4.7	6.0
cyclo-Octafluorobutane	C_4F_8	weight percentage	3.7	8.7	16.1
Soot	C_n	weight percentage	0.8	0.5	0.4

After Refs. [4, 6].

The main products of PTFE pyrolysis as a function of temperature obtained in a fluidized-bed reactor are given in Table 3.1 [4]. In the absence of oxygen, pyrolysis of PTFE at temperatures below 600 °C yields perfluoroisobutene (PFIB) [6], which is about 10 times more toxic than phosgene (LC_{50} < 1 ppm). The target organs of PFIB are the lungs and the liver [7]. However, PFIB formation has not been observed on pyrolysis of PTFE in air or oxygen [4, 6].

Ignition of PTFE in air occurs at specific irradiance levels of $E = 4.3$ W cm^2 or at an irradiance of H = 1 kJ cm^{-2}, equalling a temperature of 630 °C [8]. PTFE burns under oxygen pressure (Limiting Oxygen Index (LOI: 96%)). Figure 3.1 depicts the burn rate as a function of oxygen pressure after Ref. [9]. Burning PTFE rods attain a conical shape with some soot at the apex. At pressures below 200 kPa, the liquid layer formed at the burning surface shows bubbles indicative of gas formation. The unsaturated fluorocarbon compounds formed on pyrolysis of PTFE (C_2F_4, C_3F_6, C_4F_8) are combustible at ambient pressure, whereas the saturated fluorocarbons formed (CF_4, C_2F_6) will not burn at standard temperature and pressure (STP) [10].

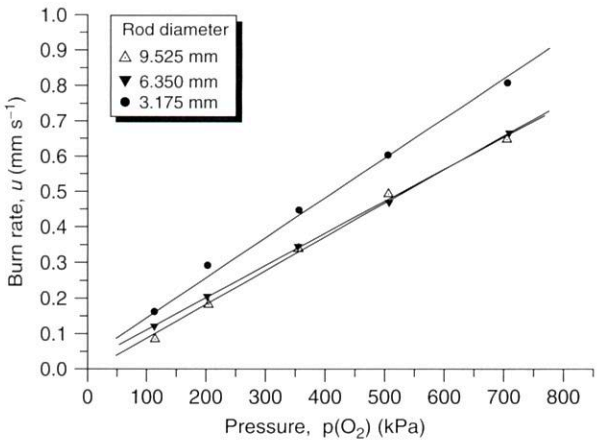

Figure 3.1 Burn rate of PTFE rods under oxygen as a function of pressure and rod diameter [9].

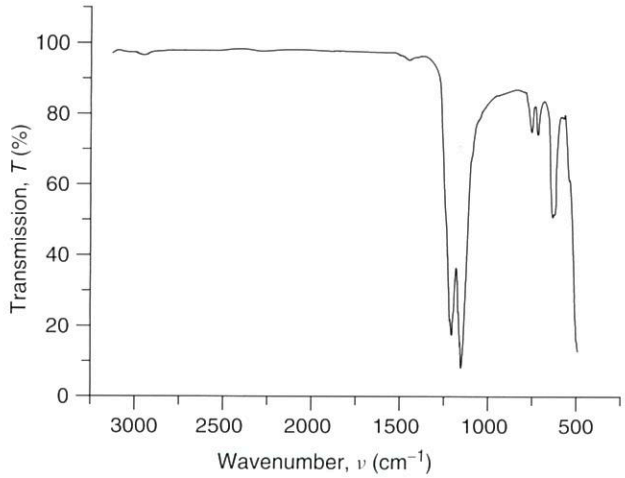

Figure 3.2 FTIR spectrum of PTFE.

Table 3.2 Characteristic IR vibrations of PTFE [11].

Mode	Wave number (cm^{-1})	Intensity
CF_2 asymmetrical stretching	1230	vs
CF_2 symmetrical stretching	1149	vs
	774	m
CF_2 scissoring	729	m
CF_2 wagging	635	s
CF_2 wagging	553	s
CF_2 rocking	520	s

The FTIR spectrum of PTFE is depicted in Figure 3.2. The characteristic vibrations are given in Table 3.2 [11].

3.2 Polychlorotrifluoroethylene (PCTFE)

Polychlorotrifluoroethylene (PCTFE) is a crystalline translucent solid polymer with a high molecular weight ranging between 10 000 and 50 000 g mol^{-1}, thus available as either viscous oil or hard plastic. It is made by polymerization of the bulk monomer or in solution, emulsion or dispersion by using free-radical starters, UV and γ-radiation. The presence of the chlorine atom improves the attractive

forces between the polymer strands, thus leading to the greatest hardness and tensile strength encountered within the group of fluoropolymers [2]. Commercial brand names for PCTFE are *Kel-F® (3M), Plaskon® (Allied Chemical Corporation), Hostaflon C® (Dyneon), Neoflon® (Daikin Industries)* and *Aclar® (Honeywell)*. Solid PCTFE has its glass transition between 71 and 99 °C and melts at 211–216 °C. It is thermally stable up to 250 °C but starts to decompose when subjected to $T > 300$ °C. However, rapid decomposition does not occur until $T > 400$ °C. The decomposition of PCTFE in air produces the monomer as the main product followed by equal amounts of CO_2, $C_2F_2Cl_2$, C_3F_5Cl and $C_2F_3Cl_3$ [12, 13]. The IR spectrum of low-molecular-weight PCTFE is given below together with the assignment of the most important vibrational bands. High-molecular weight, solid PCTFE does not exhibit the 902 cm^{-1} vibrational mode (Figure 3.3 and Table 3.3) [11, 14].

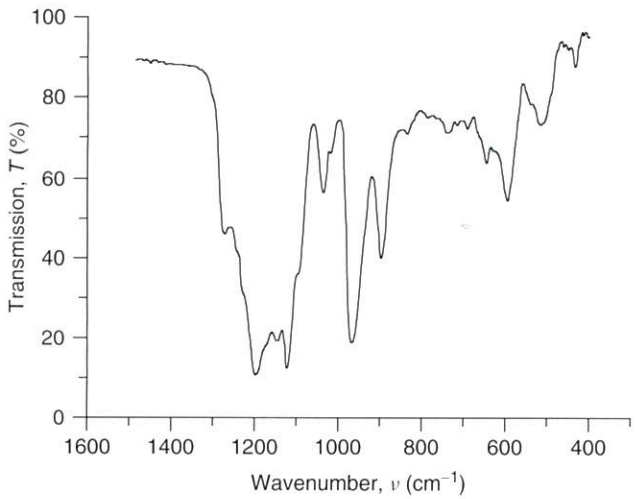

Figure 3.3 FTIR spectrum of low molecular weight PCTFE [14].

Table 3.3 Characteristic IR vibrations of PCTFE [11, 14].

Mode	Wave number (cm^{-1})	Intensity
CF stretching	1279	–
CF_2 stretching	1200	–
CF_2 stretching	1150	–
CF_2 stretching	1126	–
	1041	–
CCl stretching	970	–
	902	–
CF_2 wagging	599	–
CF_2 bending	520	–

3.3 Polyvinylidene Fluoride (PVDF)

Polyvinylidene fluoride (PVDF) (PVF_2) is made from 1,1-difluoroethylene by polymerization in bulk, solution or dispersion with starters such as peroxides or γ-radiation. Commercial PVDF products are *Kynar® (Pennwalt Corporation)*, *Solef® (Solvay)* and *Vidar® (AWK Trostberg)* [2].

Because of its alternating CF_2 and CH_2 groups, PVDF has a dipole moment (2.1 Debye), which makes it soluble in highly polar solvents such as DMF, THF, acetone and esters. PVDF is the only known polymer to occur in four different polymorphs [2]. These phases are present in the polymer at varying contents depending on the manufacture and both thermal and mechanical history of the sample. The orthorhombic phase (β-polymorph) is obtained from crystallization of PVDF from solvents. Figure 3.4 shows FTIR spectra of both orthorhombic and monoclinic (α-polymorph) phases of PVDF (Table 3.4) [15].

The density of the α-polymorph is 1.98 g cm^{-3}; amorphous PVDF has a density of 1.68 g cm^{-3}. Thus, commercial samples with a density of 1.75–1.78 g cm^{-3} have ~45% crystallinity. The α-polymorph melts at 170 °C; however, the processed polymer, because of its polymorphism, displays no sharp melting point but melts between 150 and 190 °C. The thermal decomposition becomes significant at $T > 300$ °C. Pyrolysis of PVDF yields hydrogen fluoride, the monomer $C_2H_2F_2$ and $C_4F_3H_3$ [12]. Up to 600 °C, pyrolysis also yields polyaromatic structures by cyclization of polyenic intermediates formed through HF elimination [16]. This is a particular advantage over PTFE, which is less likely to yield carbonaceous products. Thus in obscurant applications, PVDF is preferred over PTFE as a fluorine source (see Chapter 11).

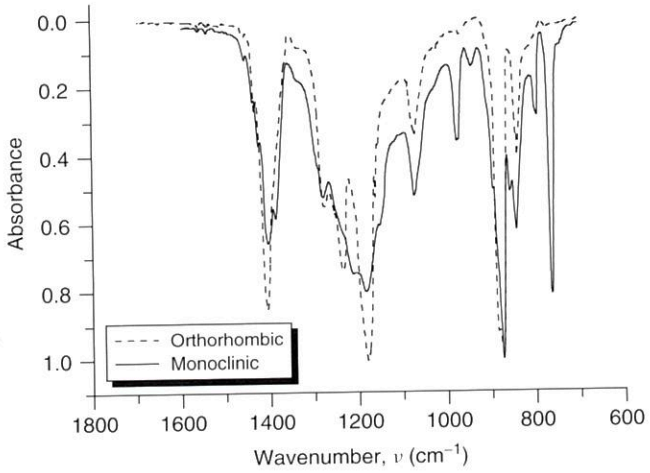

Figure 3.4 FTIR spectrum of both orthorhombic and monoclinic PVDF [15].

Table 3.4 Characteristic IR vibrations of PVDF [15].

Mode	Wavenumber (cm^{-1})	Intensity
CCH, CC, CF	1408	vs
	1385	s
	1281	s
	1240	s
CC, CCH, CCF	1180	vs
CCH	976	m
	868	vs
CCH	798	m
CCF, CF, CCC	764	vs

3.4 Polycarbon Monofluoride (PMF)

Depending on its fluorine content, polycarbon monofluoride (PMF), also known as *graphite fluoride*, is a white cream to dark grey, highly hydrophobic microcrystalline powder. It is obtained by fluorination of graphite or norite at temperatures between 400 and 700 °C [17–19]. Fluorination of less-ordered carbon materials also yields graphite fluoride, although at the expense of greater amounts of CF_4. The FTIR spectrum of a highly fluorinated sample (61% by weight F) is shown in Figure 3.5. The vibrational assignment is given in Table 3.5.

In contrast to any of the other fluorinated polymers, graphite fluoride does not melt or soften before its decomposition, which occurs slowly at temperatures above 300 °C (see DSC diagram in Figure 3.6). However, the onset of thermal

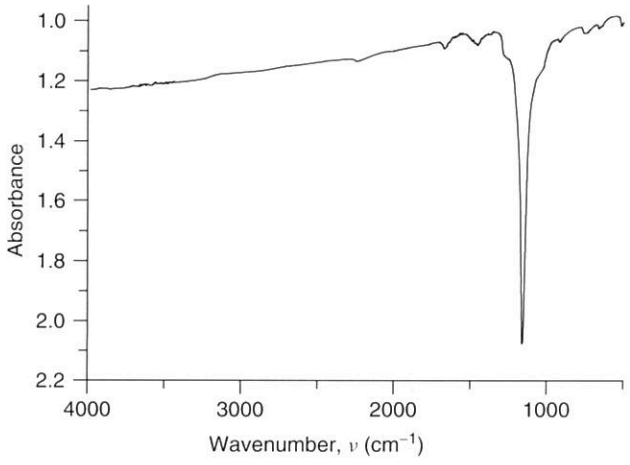

Figure 3.5 FTIR spectrum of PMF.

Table 3.5 Characteristic IR vibrations of PMF [17].

Mode	Wave number (cm^{-1})	Intensity
CF_2 symmetric stretching[a]	1350	sh
CF stretching	1219	vs
CF_2 asymmetric stretching[a]	1076	sh

[a]Owing to terminal groups at the edge of graphite sheet.

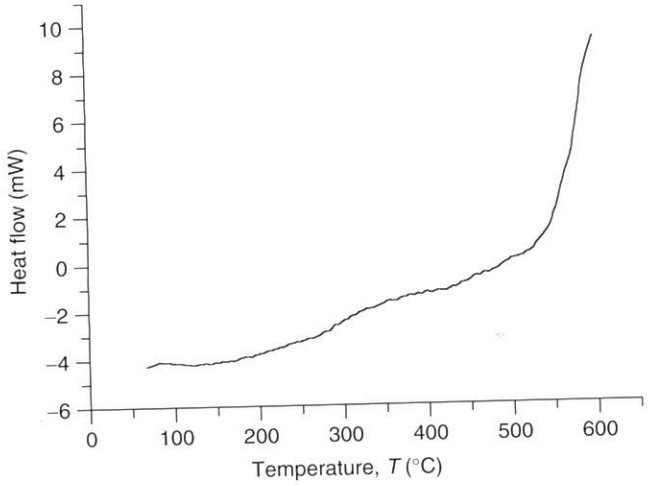

Figure 3.6 Differential Scanning Calorimetry (DSC) plot of $(CF_{0.989})_n$ at 10 K min^{-1} under 50 ml min^{-1} Ar.

decomposition with a steep slope occurs at ~500 °C for a material with $x = 0.989$. The decomposition of graphite fluoride has been investigated by Watanabe *et al.* [20–22]. They found that decomposition in both vacuum and oxygen proceeds via a similar mechanism, provided the temperature is above 588 °C. With a material containing 59.7% by weight fluorine, approximate composition $(CF_{0.937})_n$, it was found that the rate constant changes at 588 °C, indicative of change of the mode of decomposition. Below that temperature, the decomposition in oxygen proceeds very slowly and yields fluorine-containing residues, whereas at temperatures above 588 °C, no residue is obtained. Above 588 °C, the fraction of decomposed material, α, is given by the following expression known as the *Avrami–Erofeyev* equation, with k = rate constant and $n = 2$:

$$-\ln(1-\alpha) = (kt)^n \tag{3.5}$$

The decomposition of graphite fluoride under oxygen yields mainly difluorocarbene, TFE and exfoliated graphite according to the following reaction scheme:

$$\left(\frac{2x+3y}{n}\right)(CF)_n \xrightarrow[\text{Air}]{\Delta} (x+2y)C_{(\text{exp.gr})} + x\,CF_2 + y\,C_2F_4 \qquad (3.6)$$

with $n = (x + 2y)$.

3.5 Vinylidene Fluoride–Hexafluoropropene Copolymer

Vinylidene fluoride, VDF, –hexafluoropropene HFP, copolymer is a rubbery translucent milk-white polymer. Figure 3.7 shows a typical slab of the material. The monomer ratio is about 78 : 22. It is commercially available as *Viton®* *(Dupont), Fluorel FC-2175 (3M), Tecnoflon®* *(Monteflos)* or *Dai-el®* *(Daikin)*. However, these types differ slightly in composition, as is manifested in different solution behaviour in supercritical solvents [23] (see Chapter 18.3.1). In general, a VDF-HFP copolymer is soluble in ketone-type solvents. Typical molecular weights range between 1.5×10^5 and 10^6. Adiabatic compression heating in pressurized oxygen yields COF_2 and CF_4 beside CO_2 and CO, which constitute the main combustion products [13]. The thermal decomposition kinetics has been investigated in Ref. [24].

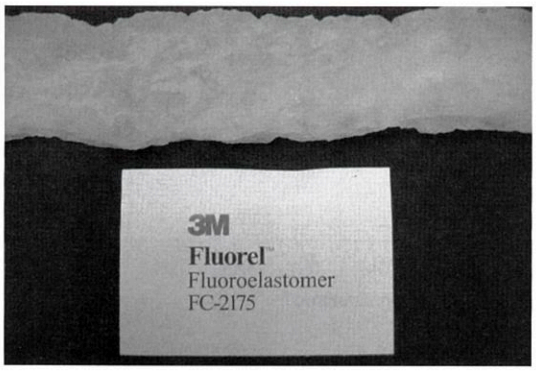

Figure 3.7 FC-2175 slab. (Reproduced with kind permission of MACH I Inc.)

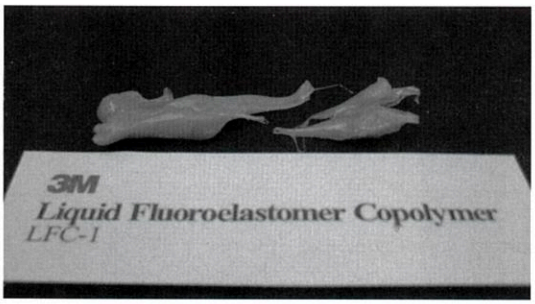

Figure 3.8 LFC-1 viscous chunks. (Reproduced with kind permission of MACH I Inc.)

ith $x = 0.989$.
Vatanabe *et al.*
n proceeds via
/ith a material
$F_{0.937})_n$, it was
e of the mode
ygen proceeds
eratures above
osed material,
feyev equation,

(3.5)

ly difluorocar-
ction scheme:

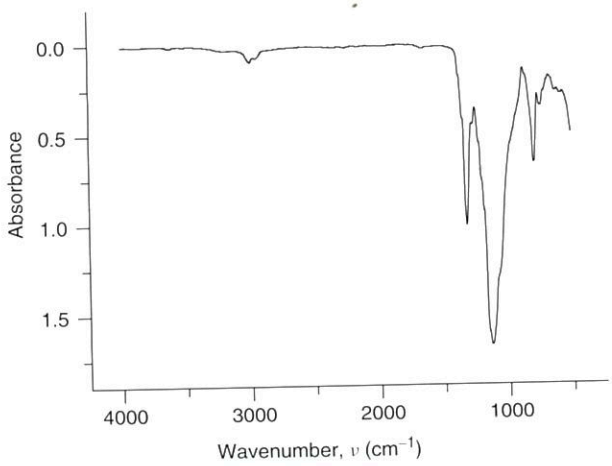

Figure 3.9 FTIR spectrum of LFC-1-polymer [25].

Table 3.6 Characteristic IR vibrations of LFC-1 [25].

Mode	Wave number (cm^{-1})	Intensity
CCH	745	w
CCH	798	m
CF	1136	vs
CF	1323	s
CH	2948	w
CH	2994	w

3.5.1 LFC-1

A special low-molecular-weight copolymer of VDF and HFP in about the same ratio as FC-2175 yields a viscous material (Figure 3.8) that enables processing energetic materials without using solvents. It is commercially available as *LFC-1® (3M)* and has a tan to brown colour. Figure 3.9 depicts the FTIR spectrum of LFC-1. Table 3.6 gives the vibrational assignment. It decomposes above 400 °C (Figure 3.10). With increasing temperature, its viscosity drops as depicted in Figure 3.11 [25].

The low shear viscosity of LFC-1 is shown in Figure 3.11.

3.6 Vinylidene Fluoride–Chlorotrifluoroethylene Copolymer

VDF–CTFE (chlorotrifluoroethylene) copolymer is a colourless granular material (Figure 3.12) that is commercially available as Kel-F 800® or FK 800® (3M) in

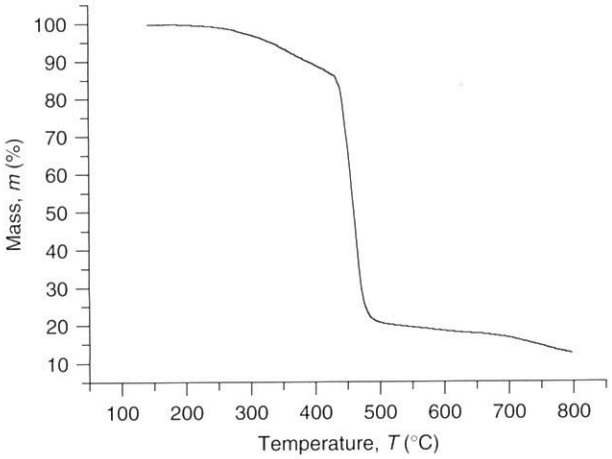

Figure 3.10 Thermogravimetry (TG) diagram of LFC-1 in air [25].

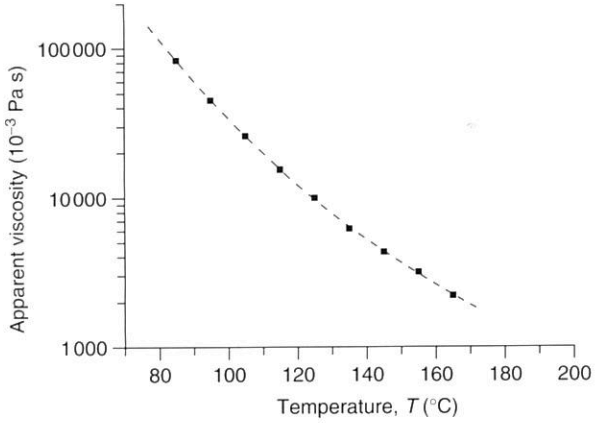

Figure 3.11 Low shear viscosity of LFC-1 [25].

Figure 3.12 FK-800 powder. (Reproduced with kind permission of MACH I Inc.)

a monomer ratio VDF : CTFE = 1 : 3. It is soluble in ketone- and acetate-type solvents, and at 10–30% by weight content, it forms clear, air-drying lacquers that are applicable by brush, dip or spray techniques. In addition, it is soluble in supercritical solvent such as CO_2 [23]. Using VDF–CTFE, compositions can be made in which binder amounts to less than 5% of the total ingredients [26]. The thermal degradation kinetics has been investigated in Ref. [24]. The thermal decomposition of a polymer with a different molar ratio of VDF : CTFE) = 4 : 1 has been investigated in Ref. [12]. The main decomposition products comprise HF, HCl, CTFE, VDF, the dimer of VDF and C_3F_5Cl.

3.7
Copolymer of TFE and VDF

TFE and VDF can be polymerized in any proportion, thus giving rise to a broad variety of products. The copolymers are obtained in either emulsion or suspension process. An approximate composition of TFE : PVDF of 20 : 80 is the eutectic point in the system, with a melting point of 120 °C. It is widely used as a technical polymer and is available under the brand names Kynar® 7200 and Kynar® SL (Pennwalt Corporation). A composition with the an approximate composition of TFE : PVDF 29 : 71) is available as Fluoroplast® 42 (Russia). Both copolymers are soluble in ketones and esters but are insoluble in alcohols and chlorinated hydrocarbons and are mainly processed via melt extrusion at temperatures between 190 and 260 °C [27, 28]. The low-wave-number FTIR spectrum of the copolymer is depicted in Figure 3.13.

Owing to the higher TFE content, Fluoroplast®-42 melts at temperatures slightly higher than the melting point (135 °C) of Kynar® 7200 (Table 3.7) and decomposes above 400 °C as is depicted in Figure 3.14 showing both DSC and TG-signal [30].

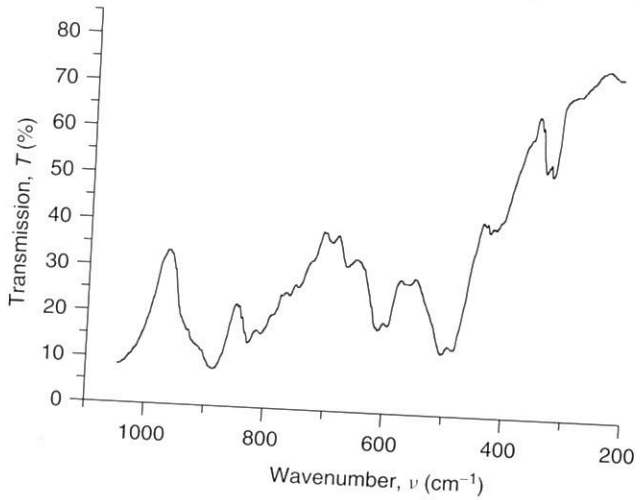

Figure 3.13 FTIR spectrum of Kynar 7200 [29].

Table 3.7 Characteristic properties of various VDF-TFE copolymer Kynar® 7200 [30, 31].

Property	Kynar® 7200	Fluoroplast®-42
Ratio of TFE : PVDF	20 : 80	29 : 71
Density (g cm^{-3})	1.88	–
Melting point (°C)	122–126	135
Heat of fusion (J g^{-1})	13–21	–
Thermal decomposition (°C)	>400	>400
Soluble in solvents	++	?
Fluorine content (wt%)	64.0	65.8

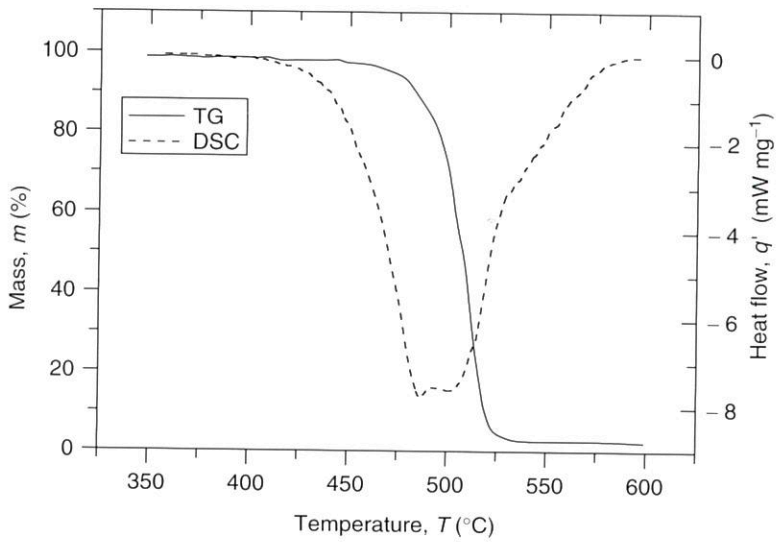

Figure 3.14 Thermoanalysis of Fluoroplast®-42 [30].

3.8 Terpolymers of TFE, HFP and VDF

Terpolymers of TFE, HFP and VDF are melt-processable fluoropolymers. They are polymerized in aqueous emulsion. Depending on the ratio of the monomers, a large number of different terpolymers are available. Figure 3.15 depicts the elastomeric region in the ternary system [28]. These materials are commercially available as *THV® (Dyneon)* [32].

The density of THV varies with composition between 1.95 and 1.98 g cm^{-3}.

Table 3.8 gives information on the principal properties of a series of commercially available Terpolymers, THV.

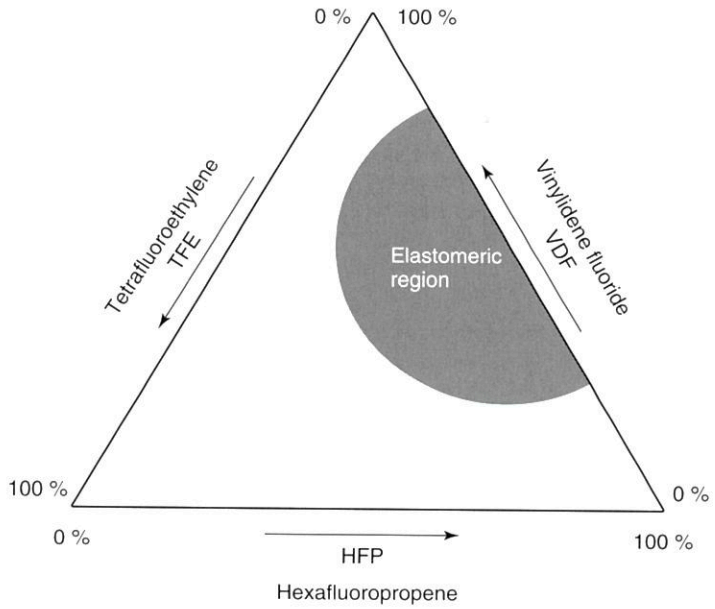

Figure 3.15 Elastomeric region in the ternary system TFE, HFP, VDF. (After Ref. [27].)

Table 3.8 Characteristic properties of various THV® grades [32–34].

Property	THV-200	THV-221	THV-X310	THV-400	THV-500	THV-610	THV-815
Density (g cm^{-3})	1.95	1.93	n.a.	1.97	2.00	2.04	2.06
Melting point (°C)	115–125	115	140	150–160	165	185	225
Thermal decomposition (°C)	420	370[a]	n.a.	430	440	370[a]	370[a]
Soluble in solvents	+	+	–	–	–	–	–
Hardness shore, D	44	44	n.a.	53	54	56	n.a.
Glass transition temperature (°C)	–	5	n.a.	–	26	34	36
Fluorine content (weight percentage)	n.a.	70.5	71–72	71–71	72.4	n.a.	n.a.

[a]Onset of thermal decomposition in presence of metal powders.

3.9
Summary of chemical and physical properties of common fluoropolymers

The following tables summarize the chemical and physical properties of common fluoropolymers.

Table 3.9 Characteristic properties of various fluorinated polymers [18, 31, 35].

Name	Formula	CAS-no	m_r (g mol^{-1})	F-content (wt%)	Tg (°C)	Mp (°C)	Dp, air (°C)
PTFE	$(C_2F_4)_n$	9002-84-0	100.016	76.0	–	328, 340	>400
PCTFE	$(C_2ClF_3)_n$	9002-83-9	116.470	48.9	71–99	211	>400
PVDF	$(C_2H_2F_2)_n$	24937-79-9	64.038	59.4	−40	154–184	350
Viton A	$(C_2H_2F_2)_n$ $(C_3F_6)_m$ $n = 3.5, m = 1$	9011-17-0	374.145	66.0	−27	–	>400
FK-800	$(C_2H_2F_2)_n$ $(C_2ClF_3)_m$ $n = 1, m = 3$	9010-75-7	413.445	50.6	28–38	105	–
PMF	$(CF_x)_n$	11113-63-6	31.01	61.3	n.a.	n.a.	610

Name	ρ (g cm^{-3})	melting enthalpy, $\Delta_m H$ (kJ mol^{-1})	enthalpy of formation, $\Delta_f H$ (kJ mol^{-1})	specific heat, Cp (J g^{-1} K^{-1})	thermal conductivity, τ (W k^{-1} m^{-1})	Limiting Oxygen Index LOI (% O_2)
PTFE	2.20	3.6	−809	1.020	0.024	99.5
PCTFE	2.10–2.13	4.659	–	0.835	–	99.5
PVDF	1.75–1.80	5.966	–	1.26–1.42	0.1–0.13	43.6
Viton A	1.82–1.85	0.3–0.7	−2784	–	0.226	31.5
FK-800	2.02	2.5	−2418	1.3	0.053	–
PMF	2.65	n.a.	−196	0.89	–	–

Abbreviations: m_r, molecular weight; Tg, glass-transition temperature; Mp, melting point; Dp, decomposition temperature.

References

1. Gangal, S. (2000) *Fluorine-Containing Polymers, Polytetrafluoroethylene, Kirk-Othmer Encyclopedia of Chemical Technology*, Wiley-VCH Verlag GmbH.
2. Carlson, D.P. and Schmiegel, W. (2000) *Fluoropolymers, Organic, Ullmann's Encyclopedia of Industrial Chemistry*, Wiley-VCH Verlag GmbH.
3. Arai, N. (1979) Transient ablation of Teflon in intense radiative and convective environments. *AIAA J.*, **17**, 634–640.
4. Simon, C.M. and Kaminsky, W. (1998) Chemical recycling of polytetrafluoroethylene by pyrolysis. *Polym. Degrad. Stab.*, **62**, 1–7.

5. Baker, B.B. and Kasprzak, D.J. (1993) Thermal degradation of commercial fluoropolymers in air. *Polym. Degrad. Stab.*, **42**, 181–188.
6. Arito, H. and Soda, R. (1977) Pyrolysis products of polytetrafluoroethylene and polyfluoroethylenepropylene with reference to inhalation toxicity. *Ann. Occup. Hyg.*, **20**, 247–255.
7. Patocka, J. and Bajgar, J. (1998) Toxicology of perfluoroisobutene, *ASA Newsl.*, **5**.
8. Lyon, R.E. and Quintiere, J.G. (2007) Criteria for piloted ignition of combustible solids. *Combust. Flame*, **151**, 551–559.
9. Ladouceur, H.D. (2005) An overview of the known chemical kinetics and transport effects relevant to Mg/PTFE combustion. 2nd International Workshop on Pyrotechnic Combustion Mechanisms, Pfinztal Germany, June 27.
10. Matula, R.A., Orloff, D.I. and Agnew, J.T. (1970) Burning velocities of fluorocarbon-oxygen mixtures. *Combust. Flame*, **14**, 97–102.
11. Liang, C.Y. and Krimm, S. (1956) Infrared spectra of high polymers. III polytetrafluoroethylene and polychlorotrifluoroethylene. *J. Chem. Phys.*, **25**, 563–571.
12. Zulfiqar, S., Zulfiqar, M., Rizvi, M., Munir, A. and McNeill, C. (1994) Study of the thermal degradation of polychlorotrifluoroethylene, poly(vinylidene fluoride) and copolymers of chlorotrifluoroethylene and vinylidene fluoride. *Polym. Degrad. Stab.*, **43**, 423–430.
13. Hsieh, F.-Y. and Beeson, H.D. (2004) A preliminary study on the toxic combustion products testing of polymers used in high-pressure oxygen systems. http://ntrs.nasa.gov/archive/nasa/casi.ntrs.nasa.gov/20100041342_20100 44104.pdf. (accessed 1 September 2011).
14. Kawano, Y. and de Araujo, S.C. (1996) Raman and infrared spectra of polychlorotrifluoroethylene. *J. Braz. Chem.*, **7**, 491–496.
15. Roth, E.P., Nagasubramanian, G., Tallant, D.R. and Garcia, M. (1999) Instability of Polyvinylidene Fluoride-Based Polymeric Binder in Lithium-Ion Cells: Final Report. Sandia Report SAND99-1164, Sandia National Laboratories, Albuquerque, New Mexico.
16. O'Shea, M.L., Morterra, C. and Low, M.J.D. (1990) Spectroscopic studies of carbons. XVII. Pyrolysis of polyvinylidene fluoride. *Mater. Chem. Phys.*, **26**, 193–205.
17. Watanabe, N., Nakajima, T. and Touhara, H. (1988) *Graphite Fluorides, Studies in Inorganic Chemistry*, Vol. **8**, Elsevier, Amsterdam.
18. Nakajima, T. and Watanabe, N. (1990) *Graphite Fluorides and Carbon-Fluorine Compounds*, CRC Press, Boca Raton, FL.
19. Kamarchik, P. and Margrave, J.L. (1976) Poly(carbon monofluoride): a solid layered fluorocarbon. *Acc. Chem. Res.*, **11**, 296–300.
20. Watanabe, N., Koyama, S. and Imoto, H. (1980) Thermal decomposition of graphite fluoride. I. Decomposition products of graphite fluoride, $(CF)_n$ in a vacuum. *Bull. Chem. Soc. Jpn.*, **53**, 2731–2734.
21. Watanabe, N. and Koyama, S. (1980) Thermal decomposition of graphite fluoride. II. Kinetics of thermal decomposition of $(CF)_n$ in a vacuum. *Bull. Chem. Soc. Jpn.*, **53**, 3093–3099.
22. Watanabe, N., Kawamura, T. and Koyama, S. (1980) Thermal decomposition of graphite fluoride. III. Thermal decomposition of $(CF)_n$ in oxygen atmosphere. *Bull. Chem. Soc. Jpn.*, **53**, 3100–3103.
23. CPIA Bulletin (1996) CPIA presents: technical area task on solubility of PEP binders in supercritical carbon dioxide.
24. Burnham, A.K. and Weese, R.K. (2005) Kinetics of thermal degradation of explosive binders Viton A, Estane and Kel-F. *Thermochim. Acta*, **426**, 85–92.
25. Hunter, R.W. (1997) A new binder ingredient for explosives. JANNAF Propellant Development and Characterization Subcommittee and Safety and Environmental Protection Subcommittee Joint Meeting, USA, pp. 113–120.
26. Mach I Inc. (2000) Product Bulletin for FK-800.

27. Arcella, V. and Ferro, R. (1997) in *Modern Fluoropolymers* (ed. J. Scheirs), John Wiley & Sons, Inc., pp. 71–90.
28. Hull, D.E., Johnson, B.V., Rodricks, I.P. and Staley, J.B. (1997) in *Modern Fluoropolymers* (ed. J. Scheirs), John Wiley & Sons, Inc., pp. 257–270.
29. Latour, M. (1977) Infra-red analysis of poly(vinylidene fluoride) thermoelectrets. *Polymer*, **18**, 278–280.
30. Tarasov, A.V., Alikhanian, A.S., Kirakosyan, G.A. and Arkhangel'skii, I.V. (2010) Chemical interaction of metallic titanium with tetrafluoroethylene-vinylidene fluoride copolymer. *Inorg. Mater.*, **46**, 1308–1312.
31. Hirsch, D.B. and Beeson, H.D. (2001) Improved test method to determine flammability of aerospace materials. Halon Options Technical Working Conference, USA April 24–26, 2001.
32. Dyneon® Fluorothermoplastic Product Comparison Guide (2009) Dyneon, Oakdale, MN.
33. Tournut, C. (1997) in *Modern Fluoropolymers* (ed. J. Scheirs), John Wiley & Sons, Inc., pp. 257–270.
34. Nielson, D.B., Truitt, R.M. and Rasmussen, N. (2005) Low temperature, extrudable, high density reactive materials. US Patent 6,962,634, USA.
35. Yeager, J.D., Dattelbaum, A.M., Orler, E.B., Bahr, D.F. and Dattelbaum, D.M. (2010) Adhesive properties of some fluoropolymer binders with the insensitive explosive 1,3,5-triamino-2,4,6-trinitrobenzene (TATB). *J. Colloid Interface Sci.*, **352**, 535–541.

6
Ignition and Combustion Mechanism of MTV

6.1
Ignition and Pre-Ignition of Metal/Fluorocarbon Pyrolants

Before ignition and steady-state combustion of a pyrolant, in the condensed phase, very often an energy release step takes place that influences both ignition and burn rate. This initial exothermal reaction is called pre-ignition reaction (PIR) [1]. PIRs have been observed with a number of different pyrolants such as $Mg/NaNO_3$ [2], Mg/BaO_2 [3], Zn/C_6Cl_6 [4], Al_3Si_2/C_2Cl_6 [5], $B/KClO_4$ [6] and finally metal/fluorocarbon systems.

It is generally assumed that the PIR yields a meta-stable species, M···AX, constituted from both metallic fuel, M, and oxidant, AX, according to the general Eqs. (6.1) and (6.2):

$$M + AX \xrightarrow{k_1} M \cdots AX \tag{6.1}$$

$$M \cdots AX \xrightarrow{k_2} MX + A \tag{6.2}$$

where M is the metal and AX any oxidizing entity, with X being an electronegative atom or atomic group.

The onset temperature of the pre-ignition reaction, T_{PIR}, is usually independent of the melting or decomposition temperature of the oxidizer but related to the thermodynamic melting temperature, T_{melt} of the metal:

$$\frac{T_{PIR}}{T_{melt}} = \alpha \tag{6.3}$$

For low melting metals such as Al, Mg and Zn, we find that $\alpha \sim 0.75 \pm 0.05$; however, with refractory fuels such as Ti and Zr, $\alpha \sim 0.45 \pm 0.05$. Table 6.1 lists T_{PIR} and onset temperature for steady-state combustion of a number of M/PTFE (polytetrafluoroethylene) pyrolants.

6.2
Magnesium–Grignard Hypothesis

With AX being a fluorocarbon, the corresponding intermediate M···AX can be considered a Grignard-type compound with a general structure shown in Scheme 6.1.

Metal-Fluorocarbon Based Energetic Materials, First Edition. Ernst-Christian Koch.
© 2012 Wiley-VCH Verlag GmbH & Co. KGaA. Published 2012 by Wiley-VCH Verlag GmbH & Co. KGaA.

Table 6.1 PIR-onset and steady-state combustion onset temperatures for selected metal/fluorocarbon pyrolants.

System	PIR (°C)	Combustion (°C)	References
Mg/PTFE	477	589	[7]
Mg/PMF	520	600	[8]
Al/PTFE	550	580	[7]
Zn/PTFE	270	420	[9, 10]
Ti/PTFE	564	580	[7]
Zr/PTFE	510	570	[11, 12]

$R_3C-Mg-F$

Scheme 6.1 Fluorocarbon Grignard(I).

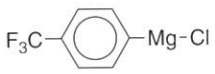

Scheme 6.2 Trifluoromethylphenylmagnesium chloride(II).

The driving force of this particular PIR reaction is the exothermic metal–fluorine bond formation. On *co*-condensation of Mg atoms and alkyl halides (R–F) at cryogenic temperatures (several 10 K), the formation of the corresponding Grignard species has been observed [13–15]. Although the formation of fluorinated Grignard species is known to be hampered for kinetic reasons, both activated magnesium [16] and magnesium anthracene ($Mg{\cdot}C_{14}H_{10}$) [17] give fluoro-Grignards in good yields. In view of this the formation of fluoro-Grignards, in thermal reactions appears a similar step. Both fluorinated and fluoro-Grignards are highly energetic species as they are prone to eliminate MgF_2 in an exothermal reaction [18]. Trifluoromethylphenylmagnesium chloride (**1**) (assessed enthalpy of formation, $\Delta_f H^\circ = -956\ \mathrm{kJ\ mol^{-1}}$ [19]; Scheme 6.2) has been even observed to explode fiercely [20, 21] according to Eq. (6.4):

$$(CF_3)C_6H_4MgCl \longrightarrow MgF_2(s) + HCl + HF + \{C_7\} + H_2 + 533\ \mathrm{kJ\ mol^{-1}} \quad (6.4)$$

The formation of **1** by Knochel reaction [22] from trifluoromethylphenylbromide with isopropylmagnesium(II) chloride in solutions >1 M can lead to a rapid increase in temperature and pressure. Hence, this reaction must be diluted down to <0.6 M to avoid catastrophic outcome [23].

The detonative potential of compositions based on Mg, benzotrifluoride and other fluorocarbons had been investigated in the 1950s; the corresponding work is still classified today (B.E. Douda, personal communication). Regardless of the known dangers of these combinations, mixtures of metal powders and benzotrifluoride have been proposed as liquid monopropellants.

At the beginning of the 1990s, it has been speculated that on combustion of Magnesium/Teflon/Viton (MTV) a similar Grignard formation step could take place [24]. For this purpose, Davis had investigated the gas-phase reaction of Mg with CH_3X, C_2H_3X (X = Cl, F) and C_2F_4 at high level of theory. He showed that all

Table 6.2 Activation energy (E_a) (kJ mol^{-1}) for Mg insertion into C–F bond of CH_3F, C_2H_3F and C_2F_4 and reaction enthalpy for Grignard formation step.

Fluorocarbon	Activation energy		Reaction enthalpy	
	SCF[a]	MP2[b]	SCF[a]	MP2[c]
CH_3F	49.5	28.5	179.1	–
C_2H_3F	56.5	25.4	168.6	226.7
C_2F_4	58.2	19.0	222.1	264.4

[a] SCF/6-31G**. Self consistent Field
[b] MP2/6-31G**//SCF/6-31G**. Møller-Plesset, MP
[c] MP2/6-31G**//MP2/6-31G**.
After Refs. [25–27].

Table 6.3 Calculated harmonic vibrational frequencies for C_2F_3MgF [27, 28].

Assignment	Wavenumber, ν (cm^{-1})	Intensity (km mol^{-1})
C–Mg–F	154	75
	178	79
	267	21
C–Mg	338	6
	374	8
	549	4
	655	12
	688	1
Mg–F	839	151
C–F	1098	50
C–C–F	1237	205
C–C–F	1439	196
C=C	1928	339

these reactions would exhibit sufficiently low activation energies and considerable exothermicity to allow under combustion conditions (Table 6.2) [25–27]. Table 6.3 lists the calculated vibrational frequencies for the calculated specie C_2F_3MgF [27], the structure of which is shown in Figure 6.1.

Davis also compared different possible reaction products formed in the reaction between difluorocarbene – a major high-temperature pyrolysis product of PTFE – and both $Mg(^1S)$ and $Mg(^3P)$. From his observations, a similar Grignard species appears energetically favoured together with a carbene-type species [24].

Thermal ignition of MTV is understood to start in the condensed phase with heat release by either Grignard-type reaction of Mg with molten PTFE (Eqs. (6.5)

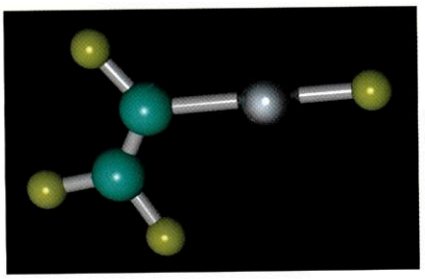

Figure 6.1 Calculated structure of C_2F_3MgF at SCF 6-31G(d) level [28] C = green, F = yellow, Mg = silver.

and (6.6)) or fluoridation of Mg with any reactive fluorocarbon specie formed by the decomposition of PTFE or Viton (Eq. (6.7)) [4]:

$$m\,Mg + (C_2F_4)_n \longrightarrow (CF_2{-}C(F){-}Mg{-}F)_n + \text{heat} \tag{6.5}$$

$$(CF_2{-}C(F){-}Mg{-}F)_n \longrightarrow (CF{=}CF)_m{-}(C_2F_4)_n + m\,MgF_2(s) + \text{heat} \tag{6.6}$$

$$Mg + 2\,R^FC{-}F \longrightarrow MgF_2(s) + 2\,R^FC + \text{heat} \tag{6.7}$$

There is good reason to assume that fluoro-Grignards form as part of the PIR in the condensed phase with Mg/PTFE and Mg/PMF (polycarbon monofluoride) [9, 29]. Samples of both Mg/PTFE and Mg/PMF heated just above their observed PIR-onset temperature (500 and 520 °C) show signals in the FTIR spectrum (Figures 6.2 and 6.3), which can be assigned to a C–Mg–F units. After further exposure of the samples at $T > 700$ °C, these structures disappear and characteristic vibrations for MgF_2 are seen in both samples.

The heat released in these steps further supports decomposition of the fluorocarbon and melting the Mg. Once sufficient gaseous fluorocarbons are released,

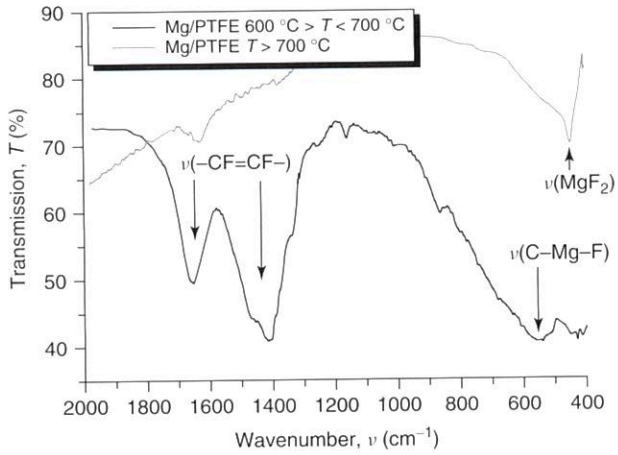

Figure 6.2 FTIR spectra of Mg/PTFE pyrolant and residues at 600 and 700 °C each [29].

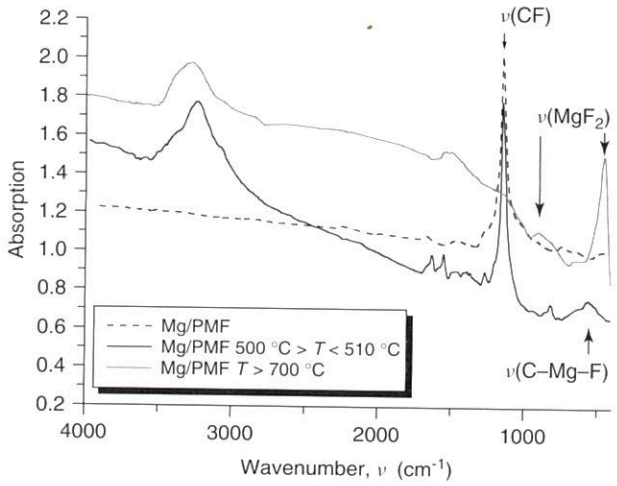

Figure 6.3 FTIR spectra of Mg/PMF pyrolant and residues at 510 and 700 °C each [9].

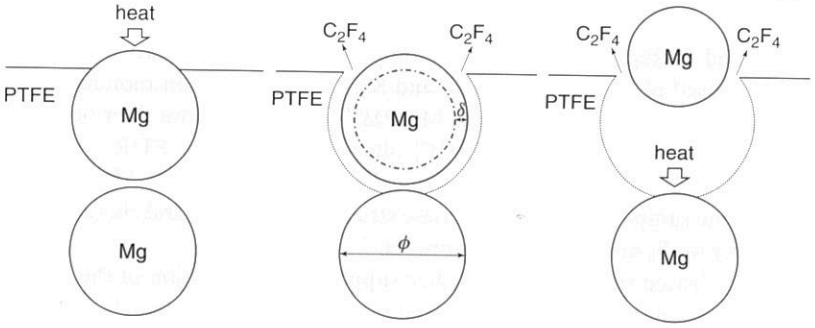

Figure 6.4 Schematic processes in the condensed phase after [35].

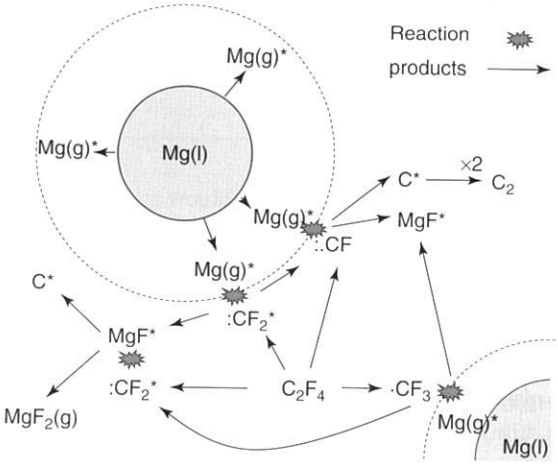

Figure 6.5 Schematic processes in the anaerobic gas phase.

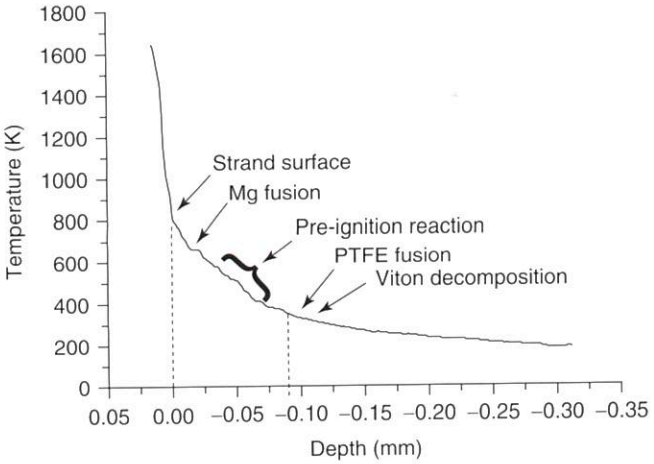

Figure 6.6 Mean-temperature profile for MTV pyrolant (30/70/3) with 22 μm Mg particles and 25 μm PTFE particle size, at 1 MPa pressure with data. (From Refs. [30–32].)

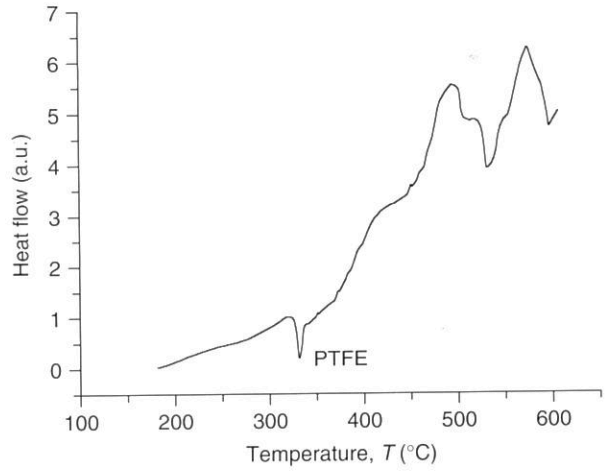

Figure 6.7 DSC for Mg/PTFE pyrolant (30/70) with 45 μm Mg particles and 5 μm PTFE particle size, at 0.1 MPa pressure.

embedded Mg particles are ejected (Figure 6.4) and react adjacent to the surface in the gas phase (Figure 6.5) as is evident from both high-speed photography and UV–VIS spectroscopy (Chapter 9). These reactions yield a heat feedback to the burning surface that, in turn, will accelerate the decomposition of PTFE and fusion of Mg until steady-state conditions are reached.

A typical temperature profile of a burning MTV strand [30–32] at 1 MPa pressure is shown in Figure 6.6. Below the surface, the strand temperature decreases

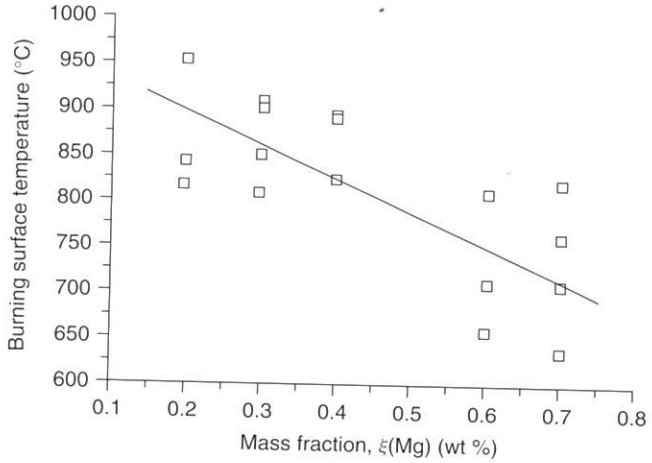

Figure 6.8 Effect of stoichiometry on surface temperature at 1 MPa. (After Refs. [30–32].)

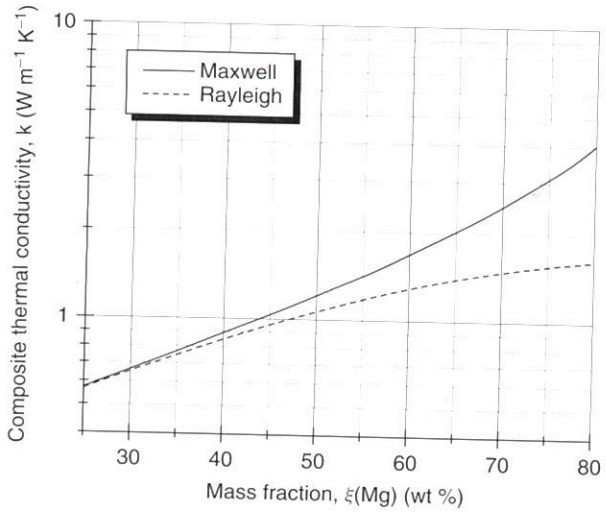

Figure 6.9 Thermal conductivity of Mg/PTFE based on either the Maywell or Rayleigh model [33].

following an exponential law. A few discontinuities are related to the fusion of Mg and heat release by PIR. Below ~300 °C, inert heating is assumed, thus not leading to any enthalpy effects. The steep rise of temperature above 800 °C is indicative of the hot gas phase above the surface. The surface temperature profile of the combustion flame has been studied as a function of both stoichiometry and pressure. The PIR of Mg/PTFE (30/70) is obvious from the DSC plot shown in Figure 6.7.

The grain surface temperature shows influence by both pressure and temperature.

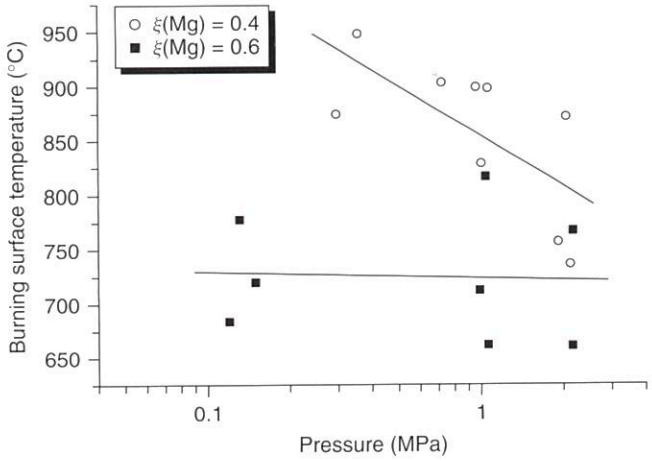

Figure 6.10 Influence of pressure on surface temperature of two different MTV pyrolant grains. (After Refs. [30–32].)

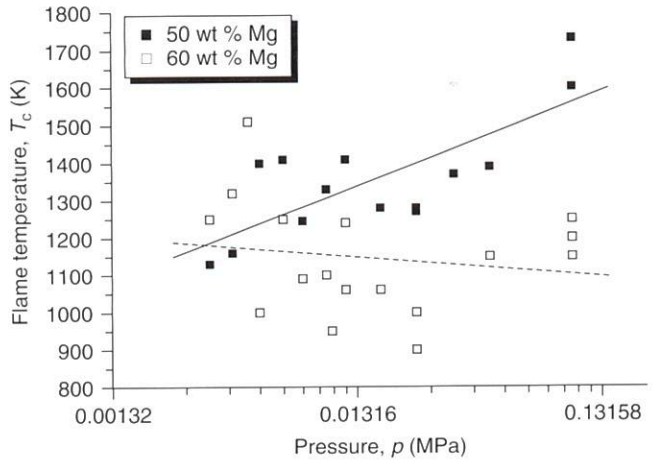

Figure 6.11 Influence of pressure on gas-phase temperature of Mg/PTFE above surface. (After Ref. [34].)

The effect of stoichiometry on the strand surface temperature is shown in Figure 6.8. It shows a temperature decrease with an increase in Mg content. This can be related to increased composite thermal conductivity (Figure 6.9), which effects faster dissipation of heat. At stoichiometries about 60 wt% Mg and above, the surface temperature scatters around the fusion temperature of magnesium (660 °C).

The influence of pressure on the temperature is less distinct. At ξ(Mg) = 60 wt%, the temperature is not affected largely by pressure changes between 0.1 and 2 MPa and scatters about 650–800 °C. In contrast, the strand surface temperature of a grain with lower Mg content (40 wt%) displays decreasing temperature with increasing pressure (Figure 6.10). This could be indicative of a Le Chatelier-type

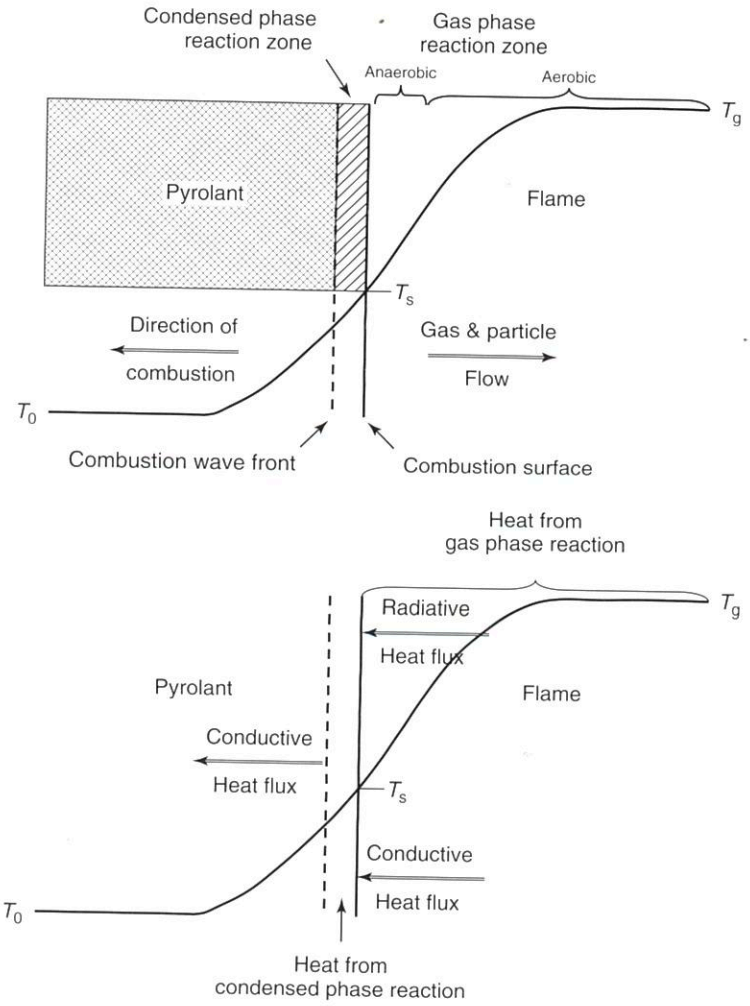

Figure 6.12 Modified qualitative structure of a pyrolant combustion wave. (After Cudziło [36].)

effect on the decomposition reactions of PTFE according to formal Eq. (6.8);

$$(C_2F_4)_n \longrightarrow n\,C_2F_4\uparrow, \quad \Delta S < 0 \tag{6.8}$$

Figure 6.11 depicts the influence of both pressure and Mg content on the temperature of the gas phase just above the burning surface determined with W/Re thermocouples [34]. With 50 wt% Mg, a decrease in temperature is seen with decreasing pressure. However, at 60 wt% Mg, the gas-phase temperature that scatters about 1200 K seems unaffected by pressure in the range between 0.003 and 0.1 MPa [1–3]. Even though the absolute temperatures are underestimated with this method (Chapter 9), the general trend should hold valid.

Figures 6.10 and 6.11 show that the thermal equilibrium of fuel-rich pyrolants is less affected by pressure than that of fuel-lean grains, which explains the lower pressure exponents of fuel-rich grains as we will discuss later.

In summary, the combustion of MTV pyrolant is determined by processes in both gas and condensed phase. Cudziło [36] has proposed a combustion wave structure for MTV. In the pyrolant, an inert temperature increase occurs that is caused by heat conduction from the adjacent condensed-phase reaction zone. In this zone, the decomposition of the fluorocarbon occurs and initial reaction with magnesium takes place (Figure 6.12), giving rise to a further increase in the temperature. Next to the condensed-phase combustion zone is the gas-phase combustion zone that is divided into an anaerobic and aerobic part. In the former, the initial decomposition products of the pyrolant react with greater homogeneity, and in the latter, the primary combustion products mix with the atmospheric oxygen and undergo after-burn reactions, allowing for a further increase in the final temperature. The heat balance of these zones is determined by the thermal conductivity of both the condensed pyrolant, and its primary combustion products and the temperature-dependent emissivity of the pyrolant surface and the primary combustion products.

References

1. McLain, J.H. (1980) *Pyrotechnics from the Viewpoint of Solid State Chemistry*, The Franklin Institute Press, Philadelphia, PA.
2. Hogan, V.D. and Gordon, S. (1959) Pre-ignition and ignition reactions of the propagatively reacting system magnesium-sodium nitrate-laminac. *Combust. Flame*, **3**, 3.
3. Hogan, V.D. and Gordon, S. (1957) Pre-ignition and ignition reactions of the system barium peroxide-magnesium-calcium resinate. *J. Phys. Chem.*, **61** (10), 1401.
4. Gordon, S. and Campbell, C. (1955) Pre-ignition and ignition reactions of the pyrotechnic system Zn-C6Cl6-KClO4. 5th International Symposium on Combustion, The Combustion Institute, Pittsburgh, PA, p. 277.
5. Hartley, F.R., Murray, S.G. and Williams, M.R. (1984) Smoke generators. IV: the ignition of loose powder mixtures of pyrotechnic white smoke compositions containing hexachloroethane and silumin in sealed tubes. *Propellants Explos. Pyrotech.*, **9**, 108.
6. Berger, B., Brammer, A.J., Charsley, E.L., Rooney, J.J. and Wirrington, S.B. (1997) Thermal analysis studies on the boron-potassium perchlorate-nitrocellulose pyrotechnic system. *J. Therm. Anal.*, **49**, 1327.
7. Kuwahara, T., Matsuo, S. and Shinozaki, N. (1997) Combustion and sensitivity characteristics of Mg/Tf pyrolants. *Propellants Explos. Pyrotech.*, **22**, 198.
8. Koch, E.-C. (2005) Metal/fluorocarbon pyrolants: VI. combustion behaviour and radiation properties of magnesium/poly(carbon monofluoride). *Propellants Explos. Pyrotech.*, **30**, 209.
9. Koch, E.-C. (2010) Metal halocarbon combustion, in *Handbook of Combustion*, New Technologies, Vol. **5** (eds M. Lackner, F. Winter and A.K. Agarwal), Wiley-VCH Verlag GmbH, Weinheim, pp. 355–402.
10. Rozner, A.G. and Helms, H.H. (1972) Smoke generating compositions and methods of use. US Patent 3,634,283, USA.
11. Cudziło, S. and Trzciński, W.A. (2001) Calorimetric studies of metal/polytetrafluoroethylene pyrolants. *Pol. J. Appl. Chem.*, **45**, 25.

12. Cudziło, S. and Trzciński, W.A. (1999) Calorimetry studies of metal/TF pyrolants. 7e Congres International de Pyrotechnie, Brest France, June 7–11, p. 440.
13. Ault, B. (1980) Infrared matrix isolation study of magnesium metal atom reactions. Spectra of an unsolvated Grignard species. *J. Am. Chem. Soc.*, **102**, 3480.
14. Bare, W.D. and Andrews, L. (1998) Formation of Grignard species from the reaction of methyl halides with laser-ablated magnesium atoms. A matrix infrared study of CH_3MgF, CH_3MgCl, CH_3MgBr and CH_3MgI. *J. Am. Chem. Soc.*, **120**, 7293.
15. Sergeev, G.B., Smirnov, V.V. and Badaev, F.Z. (1982) Low-temperature reaction of magnesium with fluorobenzene. *J. Organomet. Chem.*, **224**, C29.
16. Rieke, R.D. and Hudnall, P.M. (1972) Activated metals. I. Preparation of highly reactive magnesium metal. *J. Am. Chem. Soc.*, **94**, 7178.
17. Beck, C.M., Park, Y.J. and Crabtree, R.H. (1998) Direct conversion of perfluoroalkanes and perfluoroarenes to perfluoro Grignard reagents. *Chem. Commun.*, 693.
18. Howells, R.D. and Gilman, H. (1975) Thermal decomposition of some perfluoroalkyl Grignard reagents. Synthesis of *trans*-1-halo- and *trans*-1-alkylperfluorovinyl compounds. *J. Organomet. Chem.*, **5**, 99–114.
19. Liebman, J.F. and Slayden, S.W. (2008) The thermochemistry of organomagnesium compounds, in *The Chemistry of Organomagnesium Compounds* (eds Z. Rappoport and I. Marek), John Wiley & Sons, Inc., Hoboken, pp. 102–130.
20. Ashby, E.C. and Al-Fekri, D.M. (1990) The reaction of benzotrihalides and benzal halides with magnesium. Synthetic and mechanistic studies. *J. Organomet. Chem.*, **390**, 275.
21. Appelby, I.C. (1971) The hazards of *m*-trifluoromethylphenylmagnesium bromide preparation. *Chem. Ind.*, 120.
22. Knochel, P., Dohle, W., Gommermann, N., Kneisel, F.F., Kopp, F., Korn, T., Sapountzis, I. and Vu, V.A. (2003) Synthese hoch funktionalisierter organomagnesiumreagentien durch halogen-metall austausch. *Angew. Chem. Int. Ed.*, **115**, 4438–4456.
23. Tang, W., Sarvestani, M., Wei, X., Nummy, L.J., Patel, N., Narayanan, B., Byrne, D., Lee, H., Yee, N.K. and Senanayake, C.H. (2009) Formation of 2-trifluoromethylphenyl Grignard reagent via magnesium-halogen exchange: process safety evaluation and concentration effect. *Org. Process Res. Dev.*, **13**, 1426–1430.
24. Davis, S.R. (1990) Theoretical and experimental study of magnesium/polytetrafluoroethylene combustion. Conference, p. 49.
25. Davis, S.R. (1991) Ab initio study of the insertion reaction of Mg into the carbonhalogen bond of fluoro- and chloromethane. *J. Am. Chem. Soc.*, **113**, 4145.
26. Liu, L. and Davis, S.R. (1991) Ab initio study of the Grignard reaction between magnesium atoms and fluoroethylene and chloroethylene. *J. Phys. Chem.*, **95**, 8619.
27. Davis, S.R. and Liu, L. (1994) Ab initio study of the insertion reaction of Mg into a C-F bond of tetrafluoroethylene. *J. Mol. Struct. (THEOCHEM)*, **304**, 227.
28. Hyperchem 8.0. (2007) *Molecular Visualization and Simulation Program Package*, Hypercube, Inc., Gainesville, FL.
29. Koch, E.-C. (2002) Metal-fluorocarbon pyrolants: IV. Thermochemical and combustion behaviour of Magnesium/Teflon/Viton (MTV). *Propellants Explos. Pyrotech.*, **27**, 340–351.
30. Kubota, N. and Serizawa, C. (1986) Combustion of magnesium/polytetrafluoroethylene. 22nd Joint Propulsion Conference, Huntsville AL, June 16–18, AIAA-86-1592.
31. Kubota, N. and Serizawa, C. (1987) Combustion of magnesium/polytetrafluoroethylene. *J. Propul.*, **3**, 303–307.
32. Kubota, N. and Serizawa, C. (1987) Combustion process of Mg/TF pyrotechnics. *Propellants Explos. Pyrotech.*, **12**, 145–148.

33. Hasselman, D.P.H. and Johnson, L.F. (1987) Effective thermal conductivity of composites with interfacial thermal barrier resistance. *J. Compos. Mater.*, **21**, 508–515.
34. Griffiths, V.S., Izod, D.C.A. and O'Sullivan, E. (1970) Some observations of some pyrotechnic compositions. 2nd International Pyrotechnics Seminar, Snowmass at Aspen, July 20–24, p. 450.
35. Kuwahara, T. and Ochiai, T. (1992) Burning rate of Mg/TF pyrolants. 18th International Pyrotechnics Seminar, Breckenridge CO, July 13–17, p. 539.
36. Cudziło, S. and Trzincski, W.A. (1998) Studies of high-energy composites containing polytetrafluoroethylene. International Annual Conference of ICT, Karlsruhe, Germany, p. 151.